12 Visual system architecture

Jonathan Winawer and Hiroshi Horiguchi

Contents

12.1 INTRODUCTION

Vision is the dominant sense in primates and gives rise to an enormous diversity of behavior. Vision is used to guide locomotion, coordinate hand movements, recognize objects and scenes, direct attention, and entrain circadian rhythms. To accomplish these many functions, the nervous system includes a sophisticated network of visual pathways and structures. The eye itself contains a great number of cell types specialized for extracting particular kinds of information from the light array impinging the retina. A large portion of the brain is used to analyze the signals from the eye, including many subcortical nuclei and about 25% of the cerebral cortex (Van Essen 2004). This chapter summarizes the visual system architecture in two parts: first, the pathways by which visual information from the eye is carried to the brain, and second, how different visual functions are distributed in cortex.

12.2 VISUAL INFORMATION FLOW FROM RETINA

12.2.1 HEMIDECUSSATION

Because of the complexity of visual system architecture, it is useful to identify a few organizing principles. One such principle is the segregation and recombination of signals at multiple stages of processing. Consider the visual image itself. A single visual scene gives rise to two distinct images, one in each eye. These two images are encoded by the two retinas and then combined into binocular representations in the brain. By first separating and then recombining the image, the visual system can extract useful information about the environment. In the following text, we describe the pathways involved in this process.

In humans and many other primates, the nerve fibers exit the eye in a bundle; the fiber bundle then splits at the optic chiasm, with about half the fibers going to each of the two hemispheres. As a result, each of the two retinal images is divided in the brain: signals from the temporal hemiretina are routed to the ipsilateral hemisphere of the brain, and signals from the nasal hemiretina are routed to the contralateral hemisphere. This splitting, called *hemidecussation*, was proposed by Isaac Newton (Figure 12.1a) (Brewster 1860). The splitting of the image presumably imposes a cost, as neighboring parts of the retinal image along the vertical midline are represented by distant structures in the brain. There is also a benefit: combining the inputs from corresponding points in the two retinas supports stereopsis and hence depth perception. In species with more lateralized eyes, there is less binocular vision, and most fibers

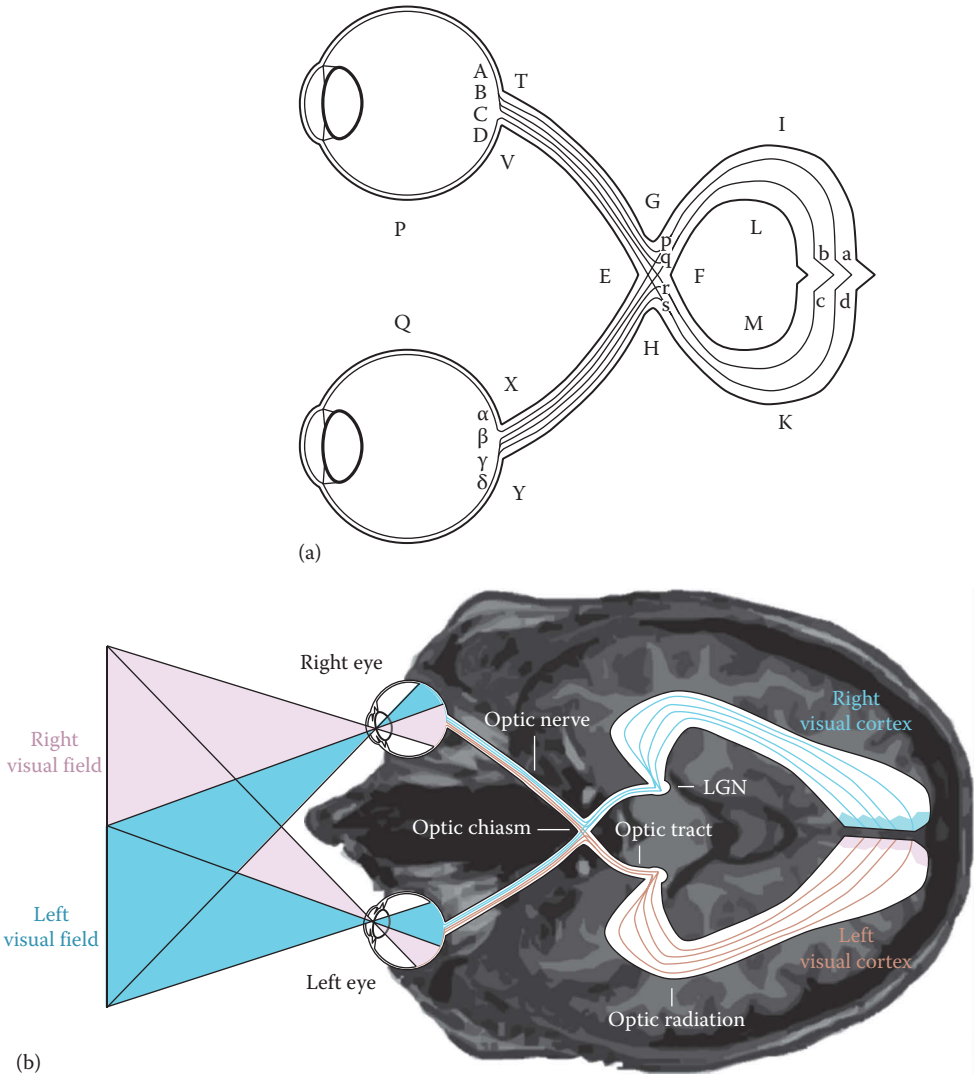

Figure 12.1 Representation of the visual fields. A key component of visual system architecture is the splitting of the visual field and the integration of the inputs from the two eyes at the optic chiasm (hemidecussation). (a) The first known diagram of hemidecussation at the optic chiasm, by Isaac Newton (Brewster 1860). Newton's early diagram of the visual pathways contains several accurate observations. First, the fibers leave the eye as a bundle, for example, ABCD leaving one eye and αβγδ leaving the other eye. Second, these fibers split at the optic chiasm, such that fibers originating from the temporal retina (AB and γδ) travel *ipsilaterally*, and fibers originating from the nasal retina (CD and αβ) travel *contralaterally*. Third, inputs originating from corresponding points of the two retinas are combined further downstream in the visual pathways (abcd). (b) A schematic of the visual pathways on an axial MRI slice shows a more modern version of Newton's drawing. The inputs from the right visual field (magenta) are routed to the left hemisphere, and the inputs from the left visual field (blue) are routed to the right hemisphere. The axons from the retinal ganglion cells hemidecussate at the optic chiasm and terminate in the LGN, where signals are then relayed to visual cortex.

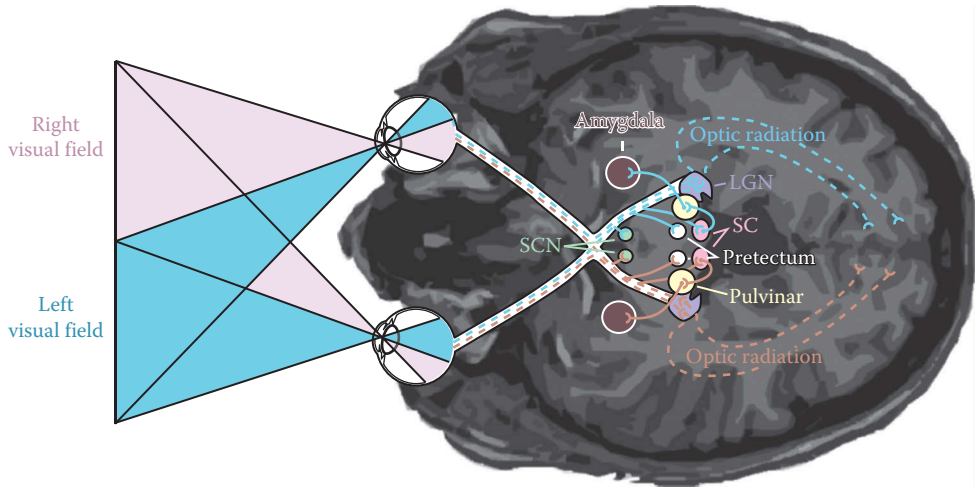

Figure 12.2 Subcortical targets of the optic nerve. Visual system architecture involves a complex network of pathways originating from the optic nerve. The largest targets of the optic nerve (~90% of fibers) are the two lateral geniculate nuclei (LGN) of the thalamus (purple), each representing one half of the visual field. The outputs of the LGN form the optic radiation, comprising the major pathway to primary visual cortex (dashed lines). Several additional nuclei are targeted by fibers branching from the optic nerve. These include the suprachiasmatic nucleus, just superior to the optic chiasm; the superior colliculus (SC), part of the midbrain; and the pretectum, just anterior to the superior colliculus. The superior colliculus projects anteriorly to the pulvinar, the largest thalamic nucleus, which in turn targets many other areas, including the amygdala. Each of the nuclei have numerous other inputs and outputs that are not depicted. The multiple pathways contribute to many functions, including perception, eye movements, pupil constriction, and regulation of circadian rhythms.

project to the contralateral hemisphere, for example, 97% in mice (Drager and Olsen 1980).

Because of hemidecussation, a lesion to the visual pathways has very different effects depending on where it occurs. A lesion peripheral to the optic chiasm (retina or optic nerve) disrupts vision through one eye. In contrast, a lesion central to the optic chiasm disrupts vision in one visual hemifield but through both eyes. Assessing whether a deficit is restricted to one eye or to one hemifield is an important tool for localizing visual disorders.

12.2.2 MAJOR SUBCORTICAL TARGETS OF THE OPTIC NERVE

All neural signals exit the eye in the optic nerve. This nerve is made up of the axons from retinal ganglion cells. There are several targets of the optic nerve (Figure 12.2), which we review in the following.

12.2.2.1 Lateral geniculate nucleus of the thalamus

About ninety percent of the axons exiting the eye terminate in the two lateral geniculate nuclei ("LGN") of the thalamus, as measured in macaque (Kandel et al. 2000, 528, Perry et al. 1984). The LGN in turn relays signals to the primary visual cortex via the optic radiation. This pathway is called the geniculostriate pathway, "geniculo" for LGN and "striate" for primary visual cortex.* The geniculostriate pathway is the dominant visual pathway in primates and supports many aspects of vision through cortical processing. In many other vertebrate species, including reptiles, birds, and rodents, the geniculostriate pathway is less dominant. For example, in mice, after lesions to this pathway, much (but not all) functional vision remains (Prusky and Douglas 2004). In humans and other primates, damage to this pathway leads to blindness in a portion of the visual field, called a *scotoma*.

The geniculostriate pathway illustrates several important principles of visual system architecture. Two of these principles—information transfer via parallel pathways and the preservation of retinotopic maps—are discussed in the following.

12.2.2.1.1 Eye-of-origin parallel pathways

The LGN is bilaterally symmetric, one in the left hemisphere and one in the right hemisphere. Each LGN comprises 6 prominent layers as visualized by histological sections in postmortem tissue. Three of the layers are ipsilateral (left eye projections to left LGN) and three are contralateral (right eye projections to left LGN), so that information from the two eyes remains segregated in the LGN and is conveyed to the brain in parallel pathways where the inputs are combined (Figure 12.3).

12.2.2.1.2 Cell-type parallel pathways

The LGN layers are also separated by retinal ganglion cell type (Figure 12.3). The primate retina contains at least 17 types of ganglion cells (Field and Chichilnisky 2007). Pathways for a few of these cell types are known. The first two layers of the LGN (ventral) receive inputs from the large, parasol ganglion cells of the retina. The large cells in these layers of the LGN are referred to as "magnocellular." The four dorsal layers of the LGN receive inputs from the smaller midget ganglion cells of the retina; the small cells in these layers of the LGN are called "parvocellular." The two sets of layers—parvocellular (layers 3–6) and magnocellular (layers 1–2)—can be distinguished in the human brain using functional MRI (Denison et al. 2014), although resolution is not yet good enough to visualize the 6 individual layers. Interdigitating between these 6 prominent layers of the LGN are the more recently discovered koniocellular layers of the

* Primary visual cortex is called "striate cortex" after the stria of Gennari, a region of myelinated axons in primary visual cortex visible to the naked eye. Cortical visual areas outside of V1 are referred to as "extra-striate."

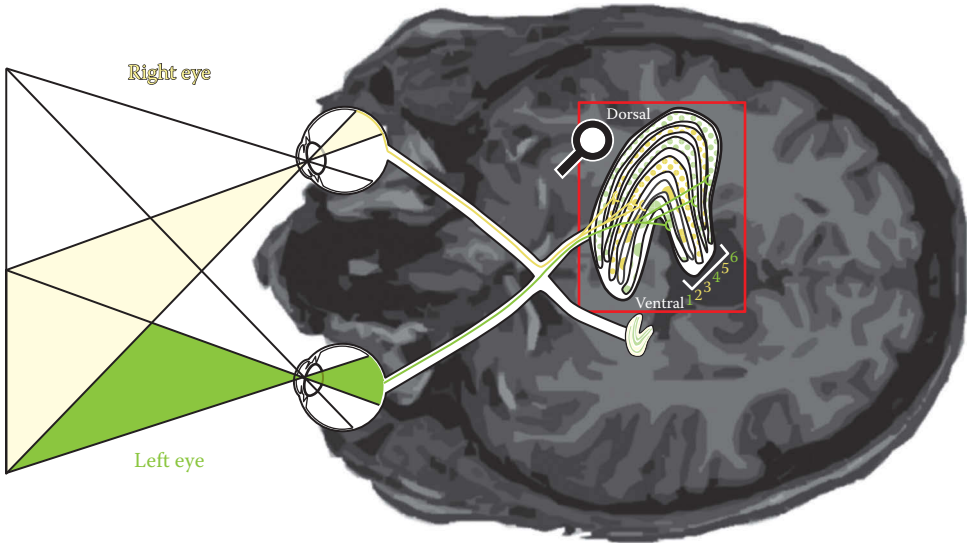

Figure 12.3 Parallel visual pathways via the lateral geniculate nucleus. A common feature of visual system architecture is the segregation and integration of neural signals transmitted in multiple parallel pathways. Signals from the left visual field, represented in the right half of the retina, are routed to the right LGN. The right LGN is shown in magnified view (red box). The magnified view is rotated relative to the underlay, exposing the dorsal–ventral axis, in order to highlight the layered structure of the LGN. The LGN layers segregate inputs by eye of origin and cell type. Layers 1, 4, and 6 (green) receive fibers from the contralateral eye, whereas layers 2, 3, and 5 receive fibers from the ipsilateral eye (yellow). Layers 1 and 2, called "magnocellular," are the targets of the parasol ganglion cells of the retina (large dotted textures), whereas layers 3–6, called "parvocellular," are the targets of the midget ganglion cells (small dotted texture). Outputs of the small bistratified retinal ganglion cells target the LGN between these layers, whose outputs comprise the koniocellular pathway (not shown). The inputs from the two eyes and the multiple cell types are combined in later stages of processing in the cortex.

LGN, which receive inputs from the small bistratified retinal ganglion cells.

The parasol, midget, and small bistratified cells comprise only a small subset of retinal ganglion cell classes. Pathways for the remaining cell classes are likely to be discovered in future work. But while these are only a few of the retinal ganglion cell classes, they comprise the vast majority of the retinal ganglion cells. The midget cells alone account for most of the ganglion cells in the human retina—about 45% in the periphery and 95% in the central retina (Dacey 1993).

12.2.2.1.3 Retinotopic maps

Just as there is organization between layers of the LGN (segregation by cell type and eye of origin), there is also organization within each layer. Organization within the layers embodies a second principle of visual system architecture, namely, preservation of the *retinotopic map*. Although the retinotopic map is not perfectly preserved within the optic nerve (Fitzgibbon and Taylor 1996, Horton et al. 1979), it is reconstituted in the LGN. Neighboring cells within a single layer of the LGN receive inputs from nearby retinal ganglion cells. While the retinal topology is mostly preserved in the LGN, it is not perfectly preserved, and the scale is significantly changed. For example, the LGN map splits the retinal image in two parts due to hemidecussation. The left LGN represents only the left half of the two retinas (right visual field), and the right LGN only the right half of the two retinas (left visual field). The LGN map also differs from the retina in that the foveal representation is greatly exaggerated in the LGN. For example, in macaque, the central 2.5° in the retina (less than 0.1% of the retinal image) projects to 10% of the LGN neurons (Connolly and Van Essen 1984, Schneider et al. 2004). Hence, an image from the retina visualized on the LGN will appear distorted in several ways. It will be split into two and larger in the center. Nonetheless, it is an image, as neighboring points in the LGN come from neighboring points in the retina. As we shall see later, the retinotopic map is preserved in many additional structures throughout the visual pathways.

12.2.2.1.4 Function of the LGN

The LGN is often described as a relay station because it receives inputs from the retina and sends outputs to the cortex. The functional properties of neurons in the LGN are not known to differ in a dramatic way from those in the retina. For example, in cat and macaque, the receptive fields tend to have center-surround organization, either with an excitatory center and inhibitory surround or vice versa, similar to receptive fields of retinal ganglion cells (Kandel et al. 2000). Rather than transforming the functional signals in a qualitative way, the LGN may serve other purposes. For example, it has been hypothesized to serve as a gating mechanism, allowing some signals to pass through to cortex while inhibiting other signals. This hypothesized gating mechanism is plausible because the LGN receives a large feedback projection from primary visual cortex, and this feedback could be used to control the responsivity of the LGN (Sherman and Koch 1986). Cognitive and task effects on the LGN have been measured in human neuroimaging experiments (Kastner et al. 2006), and in fact, it is estimated that 90% of the synapses in primate LGN are feedback from cortex, and only 10% feedforward from the retina. Nonetheless it is important to note that the feedforward signals, though smaller in number, drive the cells of the LGN very powerfully. Moreover, despite the lack of a known qualitative change in receptive field properties between retinal ganglion cells and LGN cells, there are quantitative changes. For example,

LGN cells have more suppressive surrounds and a different pattern of temporal responses; these changes may reflect cortical feedback or some degree of important visual analysis computed in the LGN (Sillito and Jones 2002).

12.2.3 SECONDARY PATHWAYS

While most of the projections from the eye project to the LGN of the thalamus, there are several secondary pathways that are also important.

12.2.3.1 Superior colliculus

After the LGN, the superior colliculus, sometimes called the "optic tectum," is the largest target of retinal ganglion cells, with about 10% of retinal ganglion cells terminating in the superior colliculi. Although the superior colliculus receives a small number of optic nerve fibers compared to the LGN, it is nonetheless a large number: about 100,000 nerve fibers, or 3 times more than the number of fibers in the auditory nerve. The superior colliculus is a paired structure, with one on each midbrain surface. This midbrain nucleus is a multilayered structure, with alternating layers of cell bodies and fibers. The superficial layers receive inputs from the eye and from primary visual cortex. The cells in these layers preserve a map of the retina, with an enhanced representation of the fovea. Although the superior colliculus is small (less than a cm long in each dimension), in recent years researchers have been able to visualize the retinotopic maps in living human brains using high-resolution fMRI (Katyal et al. 2010, Schneider and Kastner 2005). Each map represents the contralateral visual field, similar to the LGN and V1. Deeper layers of the superior colliculus receive inputs from extrastriate cortex, as well as other parts of the cerebral cortex including auditory and somatosensory areas. The representation from these sensory modalities is organized into a spatial map. Interestingly, the maps from these different sense modalities and from vision are in register. This organization is well suited for the superior colliculus to play a role in sensorimotor integration, coordinating inputs from various sense modalities and outputs to control eye movements (Stein et al. 2002). Outputs from the superior colliculus project both to midbrain nuclei involved in controlling eye movements and cortical areas such as the frontal eye fields.

12.2.3.2 Pulvinar

In primate, the pulvinar is the largest thalamic nucleus, with bidirectional pathways to all cortical lobes as well as subcortical regions including superior colliculus and amygdala. It receives input from the eye indirectly, via the superior colliculus, and comprises part of the extrageniculostriate pathway. Because the pulvinar is much smaller in carnivores and almost nonexistent in rodents, knowledge of the pulvinar's role in vision comes from primate research, including functional measurements and lesion studies in humans. Lesions to the pulvinar in human patients result in deficits of visual attention and awareness, consistent with evidence from nonhuman primate work implicating the pulvinar in visual attention and visual suppression during saccades (Snow et al. 2009). It is likely that the major projections to the various regions of cortex indicate a modulatory role, but the details are not understood. This pathway alone does not support high acuity, conscious vision because lesions to the primary visual pathway (geniculostriate) result in scotomas or blindness. Nonetheless, there is increasing research in the role of this important secondary pathway. The pulvinar is sometimes contrasted with the LGN: the LGN is a primary relay, transmitting information from the retina to the cortex, whereas the pulvinar is a higher-order relay, transmitting information between different parts of the cortex (Sherman 2007).

12.2.3.3 Suprachiasmatic nucleus

The visual pathways have some important functions in addition to seeing. One such function is the regulation of circadian rhythms. Human behavior and physiology fluctuate on a cycle that is approximately 24 h. The most obvious example is the sleep–wake cycle. But there are many other functions such as body temperature that follow a daily rhythm. Circadian rhythms are only approximately 24 h; signals from the environment, called "zeitgebers," are needed to keep our rhythms synchronized to the 24 h light–dark cycle. The most important *zeitgeber* is light. A major nucleus involved in coordinating circadian rhythms is the suprachiasmatic nucleus (SCN). The SCN is a paired structure located just above the optic chiasm in the hypothalamus. It contains biological pacemakers and coordinates control of bodily rhythms in conjunction with other brain areas including the pineal gland. The SCN receives direct inputs from the retina. Some of the inputs to the SCN are intrinsically photosensitive ganglion cells, a recently discovered cell type containing the pigment melanopsin (Berson et al. 2002, Provencio et al. 2000). Patients who are blind due to photoreceptor loss may still have circadian rhythms entrained to the daily light cycle, supported by melanopsin in retinal ganglion cells, which transmit signals to the SCN; in contrast, patients who are blind due to enucleation or to loss of the retinal ganglion cell layer do not entrain to the daily light cycle (Flynn-Evans et al. 2014).

12.2.3.4 Pretectum

The pretectum is a midbrain nucleus just anterior to the superior colliculus and just posterior to the thalamus. It is a paired nucleus, one per hemisphere, and it receives inputs directly from the eye. Like the SCN, the pretectum receives some of its inputs from retinal ganglion cells containing the photopigment melanopsin. The pretectum is a complex structure containing 7 subnuclei. It is involved in several basic functions, including the control of pupil size, the optokinetic reflex, and entrainment of circadian rhythms.

12.3 VISUAL CORTEX

12.3.1 GENICULOSTRIATE PATHWAY

The main route by which visual information arrives in the cerebral cortex is the optic radiation. This pathway is greatly expanded in primates. In birds and rodents, for example, the pathway through the superior colliculus—or optic tectum—is the dominant visual pathway, and not the geniculostriate pathway (Hofbauer and Drager 1985). The optic radiation develops early and is one of the first major white matter pathways in the human brain to become densely myelinated (Dayan et al. 2013, Kinney et al. 1988), changing little in macromolecular tissue properties over the lifetime (Figure 12.1 in Yeatman et al. 2014).

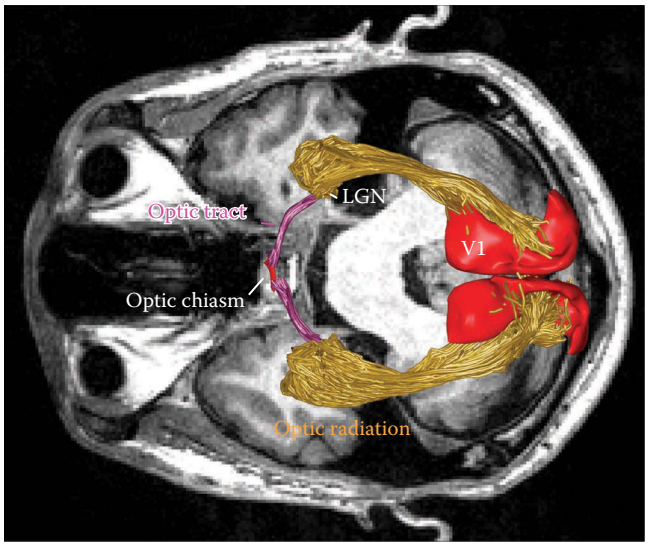

Figure 12.4 Geniculostriate pathway. The primary pathway by which the eye sends signals to the cortex is the geniculostriate pathway, consisting of the optic nerve/optic tract, the lateral geniculate nucleus, and the optic radiation. The image shows a computerized rendering of the optic tract (purple) and optic radiation (yellow), identified by fiber tractography and diffusion imaging of a living human brain. The underlay is an axial slice acquired from a T1-weighted magnetic resonance image. Image by Shumpei Ogawa.

Unlike the optic nerve, which is unidirectional, the optic radiation carries bidirectional signals between the LGN and visual cortex. The two ends of the optic radiation, the LGN and V1, are very different in sizes. V1 is about 50 times larger than the LGN (Andrews et al. 1997); each hemisphere's LGN contains about 1 million neurons, whereas each hemisphere's V1 contains about 150 million neurons, spanning 18 cm^2 (Wandell 1995). The optic radiation largely preserves the retinotopic map, so that damage to a restricted portion of the tract results in blindness in a restricted portion of the visual field. For example, one part of the optic radiation, called Meyer's loop, traverses around the occipital horn of the lateral ventricle and carries signals representing the upper visual field; a lesion to Meyer's loop results in upper field quadrantanopia (Figure 12.4).

12.3.2 V1 AND MAPS

12.3.2.1 Ocular dominance columns and parallel pathways

Primary visual cortex (V1) is located in posterior occipital cortex and distributes visual information to the rest of the brain. It receives its main input from the optic radiation, carrying signals from the LGN. As discussed in the prior section, inputs from the two eyes (but a single hemifield) are segregated into separate layers in the LGN. In V1, the inputs from these parallel pathways target interdigitated regions, called ocular dominance stripes or columns. Within each ocular dominance stripe, cells at the input layers are primarily driven by inputs originating from only one eye. These stripes can be visualized as a pattern of cytochrome oxidase activity in cortical layer IV (input layers) on the surface of a postmortem human brain of a patient who had one eye removed in adulthood (Horton and Hedley-Whyte 1984). (In the more superficial layers, the signals from the two eyes mix, and so the stripes are not clearly segregated.) In these patients, ocular dominance stripes from both eyes exist, but stripes that would receive inputs from the enucleated eyes are inactive due to lack of input (Figure 12.5).

A very different result occurs if inputs from one eye are missing or abnormal in early childhood rather than adulthood. During early childhood, signals from the two eyes compete

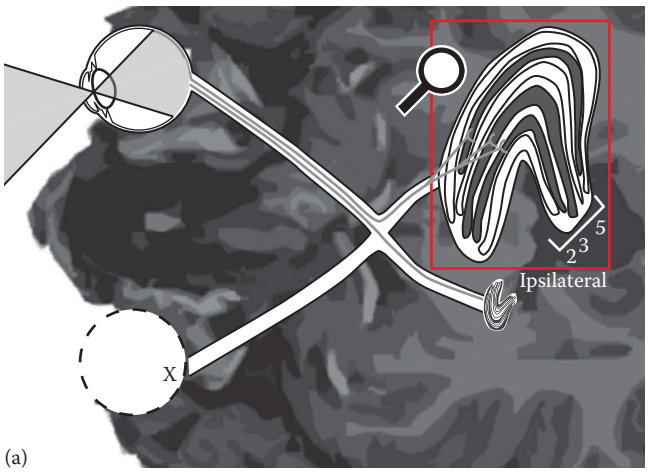

(a)

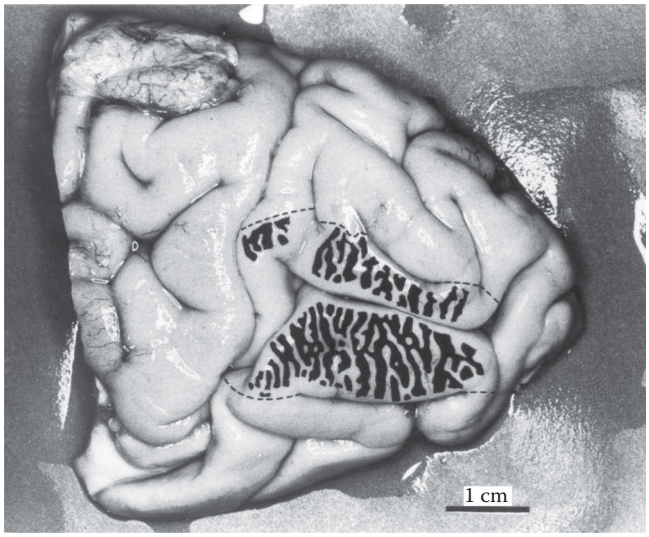

(b)

Figure 12.5 Eye-specific pathways. Eye-specific pathways in the human visual system can be studied by examining the postmortem brains of patients who had monocular enucleation earlier in life. (a) Schematic indicating eye-specific pathway in the lateral geniculate nucleus (LGN) in a patient whose left eye was enucleated (indicated by the dashed circle and "X"). Fibers from the right (intact) eye project to the ipsilateral layers in the LGN, layers 2, 3, and 5 (filled patterns in LGN). The red box is a magnified depiction of the right LGN. (b) A photograph of the right occipital lobe of a postmortem brain from a patient whose left eye was enucleated 23 years prior to his death. The dotted lines indicate the outline of primary visual cortex. The black painted regions show the locations of the right ocular dominance columns. These columns (sometimes called stripes) were identified by a method of cytochrome oxidase staining, which reveals regions of high metabolic activity. The stripes were identified on a flattened cortex and then rendered on a photograph taken of the intact occipital lobe prior to the staining and flattening procedure (Horton and Hedley-Whyte 1984). The regions between the black stripes receive inputs from a pathway originating at the enucleated eye; hence, they show lower metabolic activity. The eye-specific stripes are interdigitated throughout primary visual cortex.

for representation in V1. If signals from one eye are missing or abnormal from early infancy, then the usual pattern of ocular dominance is altered, as first demonstrated in animal experiments (Hubel et al. 1977) and later in postmortem human visual cortex (Adams et al. 2007). Even with correction of the abnormal inputs later in life, the person usually does not achieve high-quality vision through the eye with previously degraded images, likely in part due to the fact that the representation did not develop properly in V1 (Kiorpes and McKee 1999). The monocular representations in V1 are combined so that both other cells in V1 and all cells in visual areas beyond V1 are binocular. Hence, primary visual cortex is the last site in the visual processing stream in which the representations of the eyes are segregated.

12.3.3.2 Retinotopic map

The location of V1 was identified in the nineteenth century by neurologists and anatomists (Henschen 1893, Flechsig 1901). In the early twentieth century, the Japanese neuro-ophthalmologist Tatsuji Inouye first described the detailed retinotopic map in V1 (Inouye 2000). He took advantage of focal brain lesions in occipital cortex caused by bullet wounds from high velocity rifles in the Russo-Japanese war, comparing the location of the lesion in the brain to the visual field loss measured behaviorally. By combining data across many patients, each with a loss of visual field and a lesion site, he was able to derive a mapping of the visual field locations onto the visual cortex (Figure 12.6a). There were several main findings that have since been largely confirmed and described in

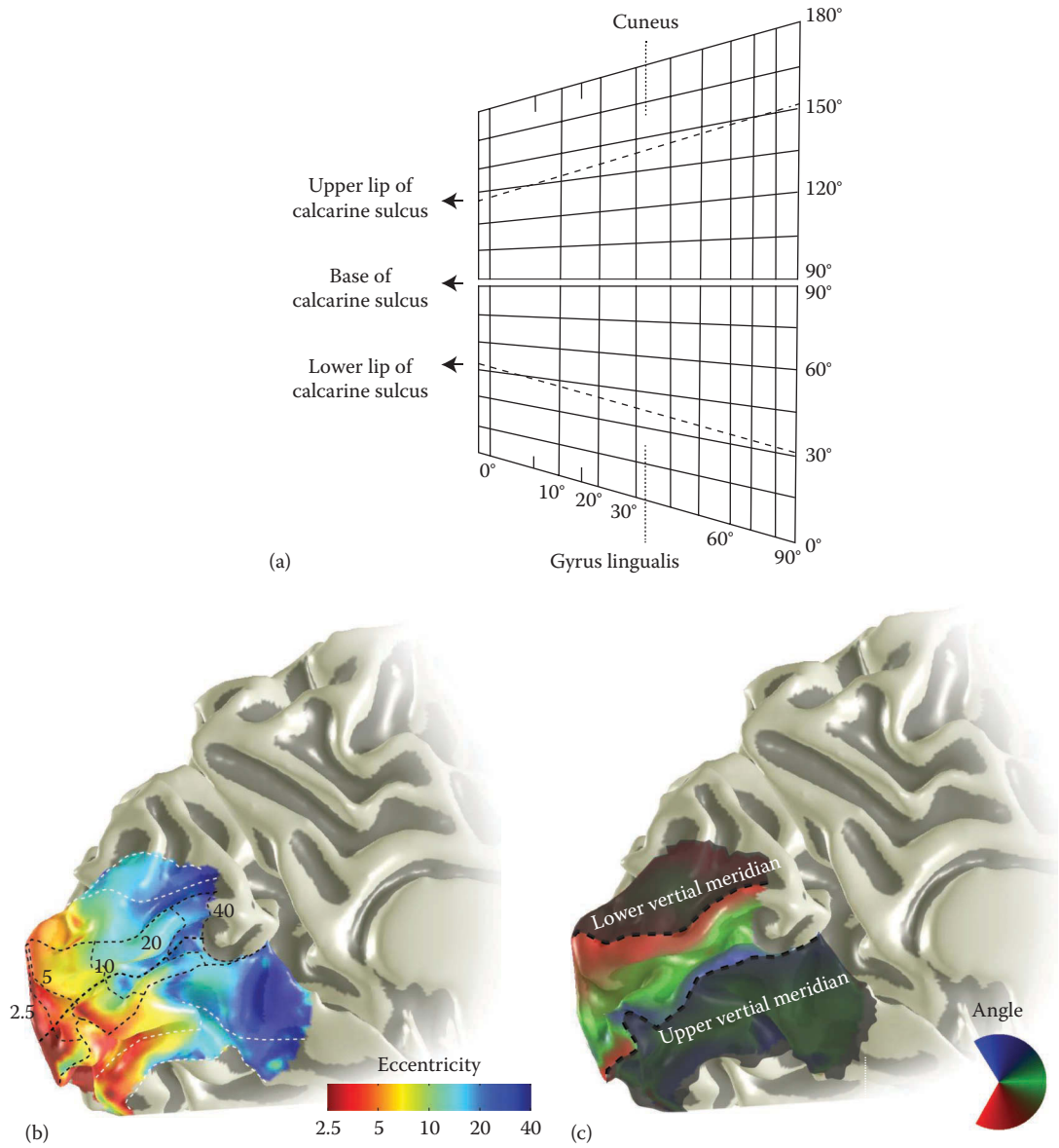

Figure 12.6 V1 retinotopic map. (a) Schematic of the visual field representation produced by Tatsuji Inouye in 1911 based on a comparison of visual field loss (scotomas) to lesions produced from bullet wounds in war (Inouye 2000). One visual hemifield is rendered in polar coordinates, with the distance from fixation (eccentricity) on the x-axis and angle representation on the y-axis. Anatomical labels indicate that the lower vertical meridian (180°) lies superior to the upper lip of the calcarine sulcus, and the upper meridian (0°) lies inferior to the lower lip of the calcarine. The horizontal representation (90°) is at the base of the calcarine sulcus. (b) Eccentricity representation in an individual observer derived from population receptive field mapping (Dumoulin and Wandell 2008) using functional MRI. (Adapted from (Wandell, B.A. and Winawer, J., *Vis. Res.*, 51(7), 718, 2011.).) Data were collected and analyzed by the authors (HH and JW). (c) Same as panel b, but showing the angle representation.

more detail. First, Inouye formulated the law of retinotopy: "neighboring points in one half of the retina are also next to one another in the corresponding principal visual area." Second, he observed that signals originating from the fovea are represented near the occipital pole and that the periphery is represented more anteriorly along the calcarine sulcus. This observation clarified views from the nineteenth century when there was uncertainty as to whether the fovea or the periphery was represented at the back of the occipital cortex (Henschen 1893). A third main finding is that the lower visual field is represented on the upper bank of the calcarine sulcus (the cuneus) and the upper visual field is represented on the lower bank of the calcarine sulcus (the lingual gyrus). Fourth, Inouye noted that the central visual field representation is greatly expanded in the cortex relative to the peripheral visual field representation, a phenomenon now called "cortical magnification."

Over the next hundred years, descriptions of the organization of primary visual cortex have become far more accurate and detailed, making it perhaps the best-studied region in the human cerebral cortex. About 10 years after Inouye's book, the V1 map was confirmed and described in more detail by Gordon Holmes and colleagues, using similar methods with patients in World War I (Holmes 1918, Holmes and Lister 1916). Decades later, lesions from strokes were identified more accurately using structural MRI and also compared to the location of visual scotomas (Horton and Hoyt 1991b) (Figure 12.6b). Currently, a detailed map of primary visual cortex can be obtained from a healthy, living individual human with less than 15 min of measurement using functional magnetic resonance imaging (Figure 12.6c). Maps of V1 derived from fMRI methods and from lesion studies using anatomical MRI show the same basic features described by Inouye and Holmes; the foveal-to-peripheral representation runs posterior-to-anterior; the lower vertical meridian is on the upper bank of the calcarine, and the upper meridian on the lower bank; and the further from the foveal representation, the less cortical territory allotted to a retinal region, so that the central 15° of the visual field occupies about half of visual cortex (*cortical magnification*, Figure 12.7). While the V1 map is generally continuous, so that adjacent locations in the retina are represented in adjacent locations in cortex (*retinotopic*), it is not perfectly continuous. Like the LGN map, there is a large discontinuity at the vertical midline, because the representation of either side of this midline projects to opposite hemispheres in the brain (*hemidecussation;* Figure 12.1).

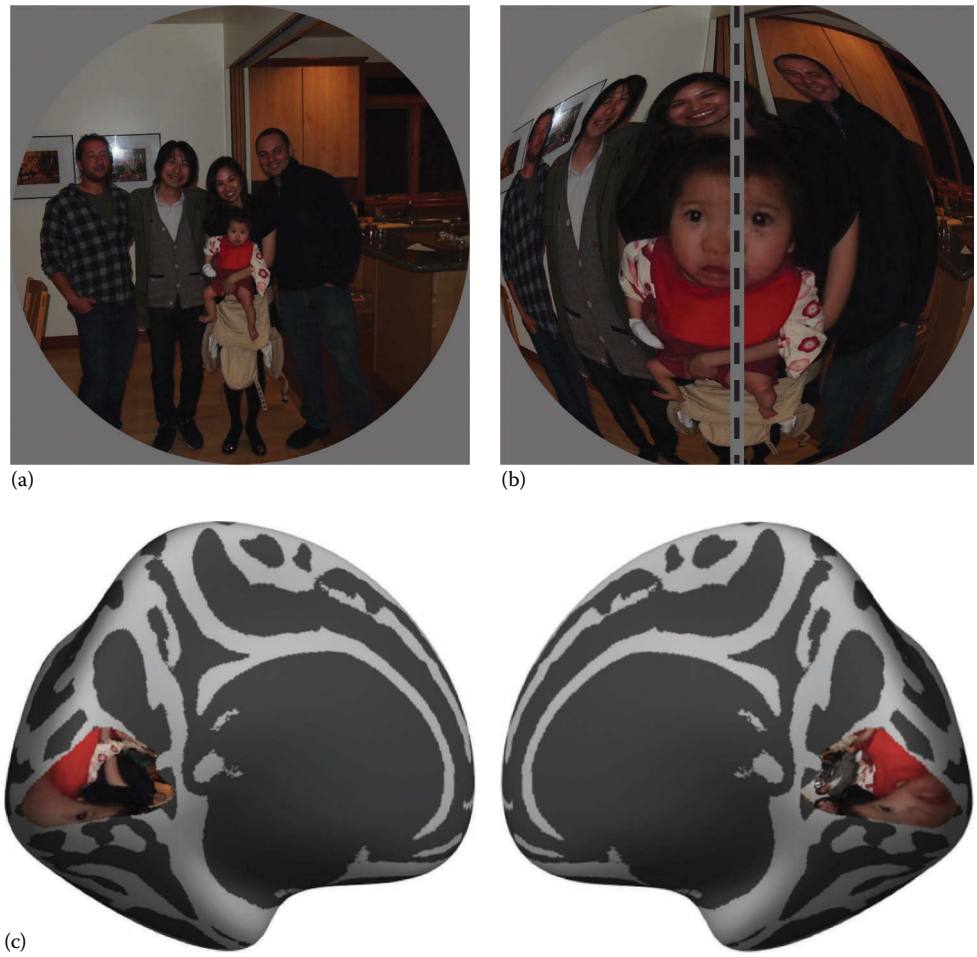

Figure 12.7 Cortical magnification. (a) A photograph simulating a retinal image. (b) The photograph in (a) was transformed to represent the approximate distortion in primary visual cortex due to cortical magnification. The center of the image is greatly expanded. The dashed line indicates that the two halves of the image are represented in the two hemispheres. (c) A more realistic rendering of the visual map in primary cortex was made by projecting the image onto a standard atlas of V1 (Benson et al. 2012, 2014), made by Noah Benson.

12.3.2.3 Measurement of retinotopic maps

A retinotopic map in visual cortex can now be measured quickly and reliably using functional MRI in healthy, awake, human subjects. In one method, a traveling wave is induced in visual cortex by presenting visual stimuli that slowly sweep across the visual field (Engel et al. 1994, Sereno et al. 1995). The method is called "traveling wave retinotopy" or "phase-encoded retinotopy" (Figure 12.8). During one measurement, a high-contrast ring slowly expands from the center of gaze (fovea) to the periphery. As the ring expands, a wave of cortical activity spreads from the posterior end of V1 to the anterior end. A single eccentricity value can be assigned to each measurement point (voxel) in the fMRI experiment by identifying the stimulus eccentricity that results in the largest fMRI response. During a separate measurement, a high-contrast wedge rotates around a circle, eliciting a wave of cortical activity that follows the angle representation in visual cortex. A single angle value is assigned to each voxel by identifying the wedge position that results in the largest fMRI signal. By combining data across the ring and wedge measurements, each voxel is assigned two coordinates, an eccentricity and angle, creating a map. Using these methods, highly detailed maps of primary visual cortex have been measured in many fMRI studies, revealing both regularity in the maps across observers (Benson et al. 2012, Schira et al. 2009) and considerable individual differences in the size (3× range, [Dougherty et al. 2003]) and precise position of the map (Dumoulin et al. 2003, Stensaas et al. 1974).

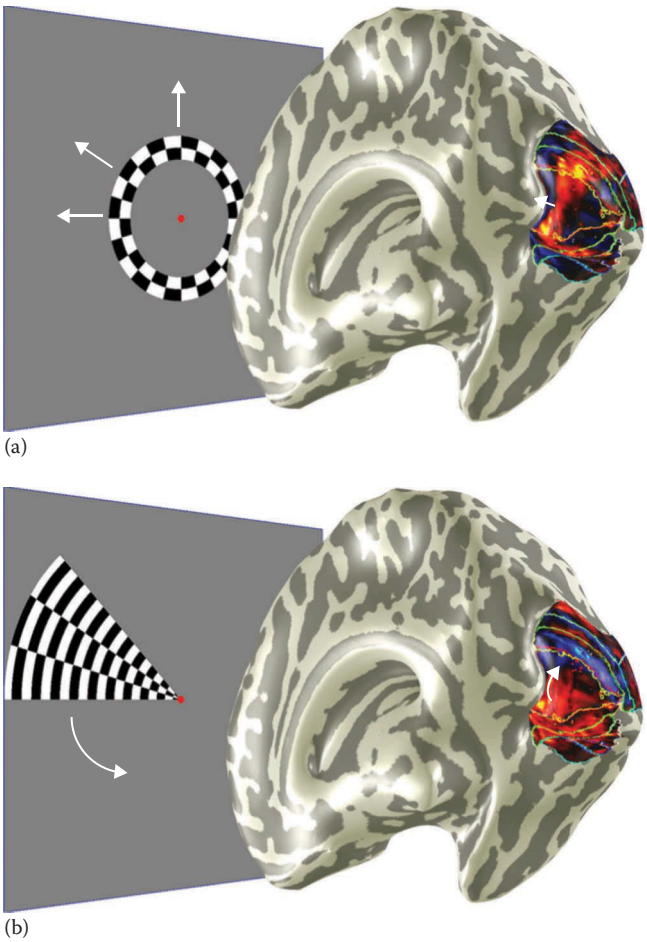

Figure 12.8 Traveling wave retinotopy. One method to obtain a retinotopic map using functional MRI is the traveling wave paradigm. (a) In one set of measurements, a ring aperture containing a high-contrast pattern cycles across eccentricities (e.g., expanding). This results in a wave of activity across the visual cortex, depicted in the rendering of an inflated right hemisphere. The pseudocolor map reveals the peak of the traveling wave at a point in time (shifted by 4 s to account for the delay in the hemodynamic signal). For each point on the cortex, the ring eccentricity that gives rise to the largest BOLD response is taken as the measurement of eccentricity for that voxel. (b) In another set of measurements, a wedge aperture containing a contrast pattern rotates around the fixation point. This results in a wave of activity across visual cortex shown on the same right hemisphere. For each point on the cortex, the wedge angle that gives rise to the largest BOLD response is taken as the measurement of polar angle for that voxel. The two coordinates, eccentricity and angle, comprise the position in visual space that correspond to a location in visual cortex.

12.3.3 MULTIPLE VISUAL FIELD MAPS: V1/V2/V3

The discovery that the cortex contains a map of the retina was a major discovery in the history of visual neuroscience. Perhaps more surprising and controversial was the set of discoveries documenting not just one, but many retinotopic maps. A second (V2), third (V3), and many more visual maps (Felleman and Van Essen 1991) have been reported in the animal literature over a period of decades. Using anatomical MRI (Horton and Hoyt 1991a) and then functional MRI (Sereno et al. 1995, Engel, Glover, and Wandell 1997), multiple visual field maps have also been shown in human, and it is now a well-accepted fact that visual cortex contains a large array of maps (Sereno and Tootell 2005, Wandell 1995, Wandell and Winawer 2011, Wandell et al. 2007, Zeki 1993) such that approximately 25% of the human cerebral cortex is estimated to be predominantly visual (Van Essen 2004). Because there are multiple visual field maps, each point in the image is represented in multiple cortical locations. In this sense, cortex is similar to the retina: just as the image is encoded in photoreceptors, bipolar cells, and multiple distinct classes of ganglion cells, each tiling the visual field, the image is also encoded in multiple cortical maps each tiling the visual field.

Using fMRI data and appropriate visualization, it is now possible to identify at least a dozen visual field maps in a single human observer from an experiment that lasts just 10–20 min. The locations of 12 such maps are shown as an example of surface rendering in the right hemisphere surface rendering (Figure 12.9). In addition to the 12 maps depicted, a number of additional maps have also been discovered, including several in parietal cortex (intraparietal sulcus [Swisher et al. 2007]) and ventral temporal cortex (parahippocampal cortex [Arcaro et al. 2009]) and anterior occipital cortex (V6 [Cardin et al. 2012, Pitzalis et al. 2006, Stenbacka and Vanni 2007]) as well as frontal cortex (Jerde and Curtis 2013, Jerde et al. 2012). With the exception of frontal cortex, the maps abut one another so that a large, contiguous region of cortex is tiled with maps. Identification of the multiple maps is generally accomplished by the same methods used to study V1, especially the traveling wave method for fMRI experiments (Engel et al. 1994, Sereno et al. 1995, Engel, Glover, and Wandell 1997). Using these methods, it is common to visualize maps on the cortical surface of the two polar coordinates of the stimulus location—angle and eccentricity—that most effectively drives the BOLD response in each voxel.

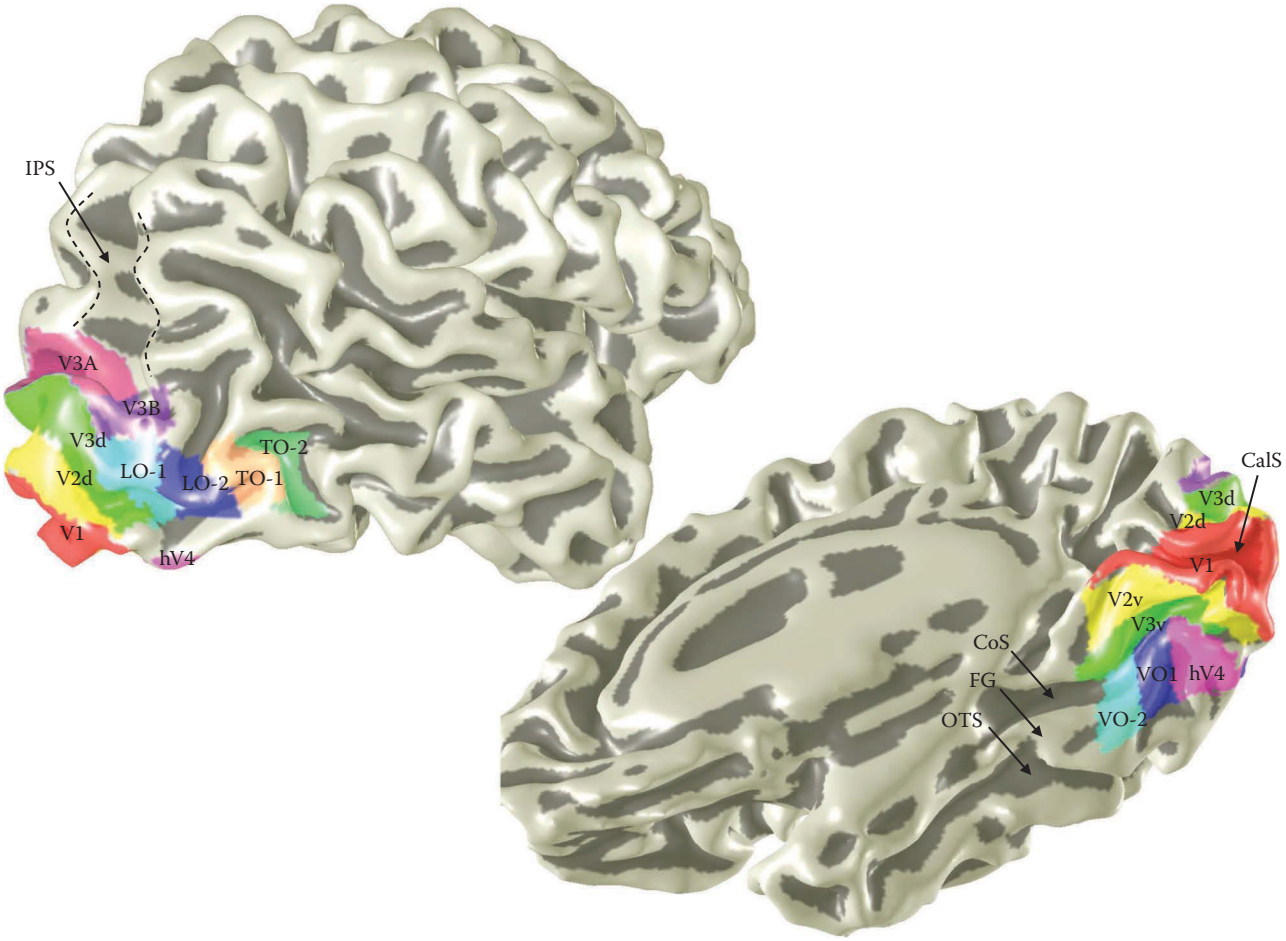

Figure 12.9 Locations of visual field maps. The locations of 12 visual field maps are indicated on the surface rendering of the right hemisphere. Two maps, V2 and V3, are each split into ventral and dorsal parts (V2v/V2d, V3v/V3d). The maps were derived from population receptive field modeling using fMRI. Several major sulci and gyri are labeled: intraparietal sulcus (IPS), calcarine sulcus (CalS), collateral sulcus (CoS), fusiform gyrus (FG), and occipitotemporal sulcus (OTS). (Reproduced from Wandell, B.A. and Winawer, J., *Vis. Res.*, 51, 718, 2011.)

A close-up view of the occipital cortex shows how these two color maps are used to identify multiple visual maps (Figure 12.10). We consider the V1, V2, and V3 maps first. The V1 map is surrounded by V2, which has an approximately horseshoe shape, and similarly, V2 is surrounded by V3. One reason these are considered separate maps is that each one—V1, V2, and V3—contains a complete representation of the contralateral visual hemifield. For this reason, borders between the maps are drawn at reversals in one of the polar coordinates. For V1, V2, and V3, the borders are reversals in the polar angle representation. One consequence of this arrangement is that the V2 and V3 maps contain a split hemifield representation, with a dorsal arm representing the lower visual quadrant and a ventral arm representing the upper visual quadrant. In contrast to the angle representation, which contains reversals at the V1/V2 and V2/V3 boundaries, the eccentricity representation is in register across several maps. This can be visualized as the large orange region at the occipital pole (foveal representation), surrounded by bands of increasing eccentricity (yellow, green, cyan, blue). Because the eccentricity map is in register across several visual field maps, and because the angle map boundaries are challenging to delineate near the foveal representation, the region at the occipital pole is sometimes referred to as the confluent fovea. The maps beyond V1, V2, and V3 are described in the following.

12.3.4 MAP ORGANIZATION

As the number of visual field maps described in the literature has grown well beyond V1, V2, and V3, to 20 or more maps, questions of large-scale map architecture become increasingly important: Are there organizing principles to the many maps? What is the scale over which visual functions are computed? How close is the homology between the human visual system and animal models? Several ideas have been advanced to explain why there are so many maps and how they are organized. These ideas are not necessarily in conflict, but rather each may highlight one or a few aspects of the cortical architecture.

12.3.4.1 Dorsal/ventral streams

One important proposal is that the maps can be separated into two processing streams, one more ventral and one more dorsal. According to this proposal, the two streams are, approximately, functionally and anatomically distinct (Ungerleider and Haxby 1994, Ungerleider and Mishkin 1982). The dorsal pathway includes a number of maps that support the representation of motion, spatial

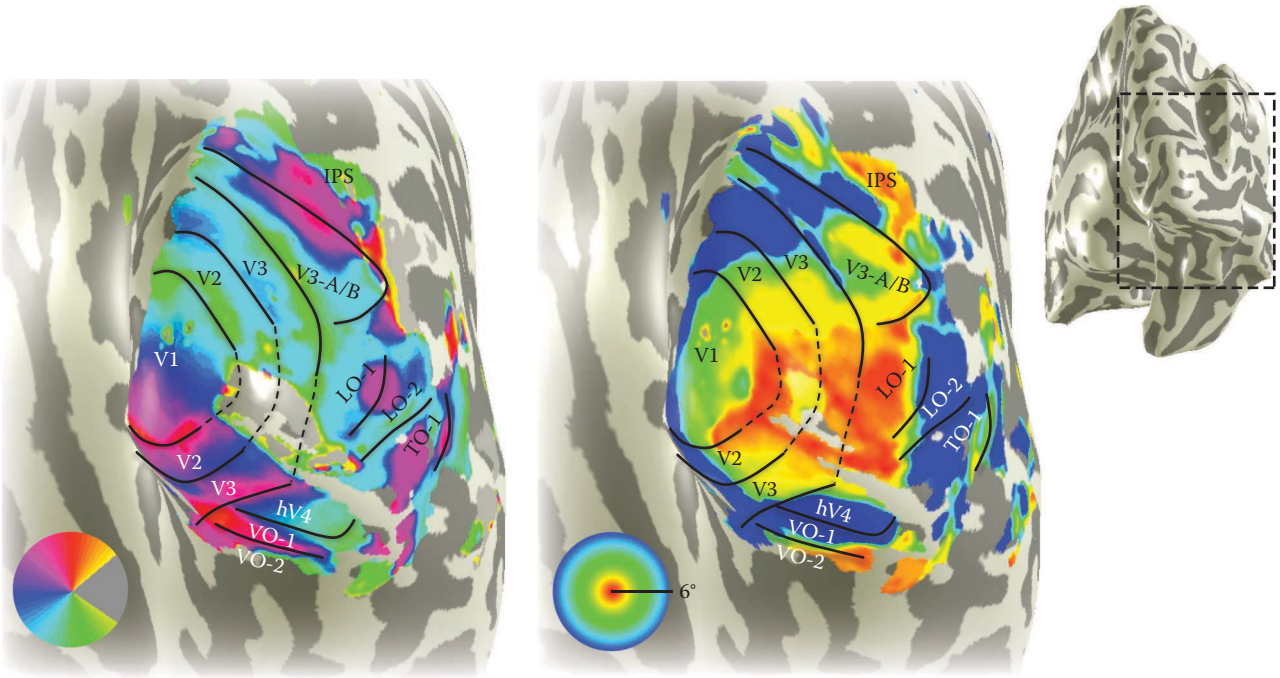

Figure 12.10 Retinotopic maps at occipital pole. The small inset on the right shows a rendering of a subject's right hemisphere, smoothed to show the sulci (dark grays) and gyri (light grays). The view is from behind the occipital pole. The dashed rectangle is a region magnified in the two main images. These images, both showing the same anatomical underlay, are overlaid with pseudocolor maps to show (a) the most effective angle or (b) the most effective eccentricity of visual stimulation for each point on the cortical surface. Data were modeled as population receptive fields in each voxel; locations are uncolored where the variance explained by the model is low. The images show a number of retinotopic maps tiling much of occipital cortex. Solid lines indicate boundaries between maps as revealed by the retinotopy data. Dashed lines interpolate over regions in which the measurements are poor, including a large region at the occipital pole where functional MRI data are obscured by a large vein (Winawer et al. 2010). (After Figure 1 in Wandell, B.A. et al., Computational modeling of responses in human visual cortex, in *Brain Mapping: An Encyclopedic Reference*, ed. A. Toga, 2015.)

location, and action. The ventral pathway includes maps involved in seeing color and form and recognizing objects and scenes. This notion is consistent with the idea of parallel pathways in the transmission of visual information, though it is important to note that the two streams are not entirely distinct. A major fiber pathway, the vertical occipital fasciculus (Yeatman et al. 2013), connects the two pathways and likely supports functions that require integrating object information (form, color, and so forth), which are action and location information. Reading, for example, requires recognizing shape and controlling eye movements.

One complication with the two-stream proposal is that the topography of human visual cortex is more consistent with three branches of visual field maps rather than two, each extending anteriorly from the early visual field maps at the occipital pole. The three streams are ventral (Arcaro et al. 2009), lateral/temporal (Amano et al. 2009), and dorsal/parietal (Swisher et al. 2007). It is not clear how the lateral/temporal maps would fit into the two-stream hypothesis.

12.3.4.2 Hierarchies and areas

A more detailed proposal is that the dorsal and ventral streams are organized as two branches in a visual hierarchy. The proposal that the multiplicity of areas forms a hierarchy is perhaps the most influential view of visual cortical architecture. The idea is an extension of the clear fact that the early visual system is hierarchical. For example, retinal ganglion cells can be said to lie above the photoreceptors and below the thalamus in a visual hierarchy, as neural encoding of light first takes place in the photoreceptors, and signals are then transmitted primarily in one direction. However, once primary visual cortex distributes visual signals to many other parts of the brain, signals from any area can, in principle, affect responses anywhere else. Hence, whether there is a hierarchy of visual areas within the cortex is an empirical question. The notion of a hierarchy of visual areas is sometimes matched to the idea the visual perception unfolds in a series of discrete steps (Riesenhuber and Poggio 1999).

By analyzing many published data sets, Felleman and Van Essen (1991) showed that the pattern of connections between visual areas in macaque monkey was mostly, though not completely, consistent with a hierarchy of several levels, where one or more visual areas could be assigned to each level. The analysis was supported by the laminar pattern of connections. Similar studies have not been carried out in human, as tracer studies are generally not available.

In Felleman and Van Essen's hierarchy, the fundamental unit is the visual area. Visual areas were identified by several criteria, including connection patterns between areas, cytoarchitecture, and retinotopy. Because retinotopy is only one of several criteria, an area as treated by Felleman and Van Essen does not always have a one-to-one relationship with a retinotopic map. Some areas may contain a partial map, some may contain multiple maps, and some may not clearly contain a map at all.

12.3.4.3 Clusters

A different hypothesis is that the visual field maps are organized as several clusters (Wandell et al. 2005). According to this hypothesis, a cluster consists of several maps, arranged semicircularly around a common foveal representation. The eccentricity bands are in register across the maps within a cluster, and the angle bands are approximately radial, though the two types of measurements (angle and eccentricity) need not be precisely orthogonal. This proposal emphasizes visual field maps as the organizing unit, rather than cytoarchitecture, cell type, or connectivity. This is important because within a single map, there may be systematic variation in cytoarchitecture, such as the cytochrome oxidase "stripes" within V2. A hypothesis is that the maps within a cluster share computational resources such as circuitry for short-term memory and timing of neural signals. Furthermore, perceptual specializations may be organized in part at the cluster level, such as motion computations with the hMT+ cluster. Evidence for cluster organization has been found in both human and macaque using fMRI (Kolster et al. 2009, Wandell et al. 2005). The cluster proposal, like the hierarchy proposal, is also consistent with the theory that distinguishes between ventral and dorsal maps.

12.3.4.4 Diffusion imaging and tractography

A central question in map organization is how the maps communicate with one another. Historically, connections between the maps have been most extensively studied with postmortem anatomical tracer studies in animal models, especially the macaque. However, it is increasingly clear that beyond V1–V3, homology between the human visual system and the macaque visual system is at best highly uncertain (Sereno and Tootell 2005). Certain maps in human, like hV4 (human V4), differ in location and topology from macaque V4 (Brewer et al. 2005, Witthoft et al. 2014, Winawer et al 2010). Other maps, such as V3B and LO-2, exist in human but might not exist in macaque at all. Hence, it is critical to measure both map organization and connectivity between maps in the living human brain. In recent years, diffusion MRI combined with computational tract tracing has enabled the study of fiber pathways in living human brains. These tools are especially good at measuring large fiber bundles, tracing their pathways, and assessing tissue properties such as macromolecular tissue volume within the tracts (Mezer et al. 2013). Currently the method is less sensitive to small, local pathways. Being able to identify pathways in the living human brain has a number of applications. For example, once identified, quantitative MRI can be used to assess tissue properties, and these can be compared across development or between subject populations (healthy/disease). Moreover, tracts can then be followed over time within an individual, such as a patient with multiple sclerosis, to evaluate disease progression. Another important application of diffusion imaging and tractography is the identification of circuits for uniquely human behavior, such as reading. The major visual pathways involved in reading have been identified with diffusion imaging and studied extensively, in the context of both development and reading disorders (Ben-Shachar et al. 2007a) (Figure 12.11).

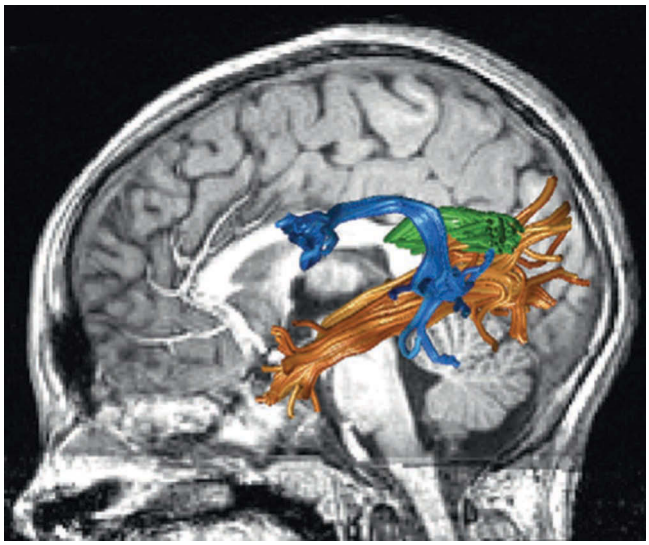

Figure 12.11 Reading circuitry. Diffusion magnetic resonance images were acquired in living human brains. The diffusion images, combined with fiber tractography, were used to identify several of the fiber bundles comprising the circuitry for reading: arcuate fasciculus (blue), inferior longitudinal fasciculus (orange), and temporal callosal projections (green) for a representative subject. The underlay is a sagittal slice from a T1-weighted image of the same subject. For the software and data used to create this image, see http://github.com/jyeatman/reading_circuits. (Reproduced from Wandell, B.A. and Yeatman, J.D., *Curr. Opin. Neurobiol.*, 23, 261, 2013.)

12.3.5 FUNCTIONAL MEASUREMENTS WITHIN MAPS AND VISUAL AREAS

A great deal of study has been dedicated to the response properties of individual neurons in primary visual cortex of cat and macaque, most famously by David Hubel and Torsten Wiesel (Hubel and Wiesel 1977). These studies, and the much more computational models that have followed, have characterized responses in visual cortex in terms of basic stimulus properties such as wavelength, contrast, orientation, and binocular disparity and in terms of computational principles such as rectification and normalization. There are many excellent reviews of the single-unit electrophysiology results from animal models, for both V1 and other visual areas (Carandini et al. 2005, Heeger et al. 1996, Maunsell and Newsome 1987, Shapley and Hawken 2002). We do not review this literature here, but instead focus primarily on studies of cortical response properties in the human visual system.

12.3.5.1 Population receptive fields

Given the large number of visual field maps in the human visual system, a natural question to ask is how the representation of the visual image differs between the maps. In the last decade, significant progress has been made in quantitative models of the fMRI signal in visual cortex. This modeling framework is often referred to as population receptive field (pRF) modeling. The word "population" indicates that the model measures responses from a population of neurons, not an individual neuron. The phrase "receptive field" is used by analogy to receptive field mapping of individual neurons, in which the brain response is expressed not in units of brain activity but in terms of stimulus properties such as contrast, position, and orientation. pRF modeling can also be fit to data from instruments other than MRI, such as the local

field potential recorded from microelectrodes in animals (Victor et al. 1994) or intracranial electrodes in humans (Harvey et al. 2012, Winawer et al. 2013, Yoshor et al. 2007).

The pRF model predicts the entire time series of a voxel in an fMRI experiment. It does so by taking images as input and predicting the BOLD response as output (or ECoG or other measurement modalities). The first generation of pRF models assumed a linear pooling of spatial contrast and built predictions based on stimulus location and not the specific pattern comprising the stimulus (Dumoulin and Wandell 2008). The model identified the position and spatial extent of the region of visual space in which stimulus contrast results in a response at the measured site (e.g., an MRI voxel). As such, the pRF model goes beyond the travelling wave approach by quantifying the extent of spatial pooling, rather than a single point. The results of pRF modeling have revealed several patterns across visual cortex (Figure 12.12). First, the scale of spatial pooling (pRF size) increases as the voxel's pRF center location is more remote from the fovea (greater eccentricity). Second, pRF size differs across visual areas. For example, the pRF size in V1 is about half that of V3, which in turn is about half that of hV4. These general patterns are consistent with decades of single-unit recording in animal models, and they provide one example of how visual representations differ across the visual field maps.

To capture further aspects of visual representation, pRF models have expanded to account for a greater number of stimulus parameters. To do so, the models have necessarily become more complex (Figure 12.13). Newer models begin with the pixels in the image rather than the spatial locations (apertures) (Kay et al. 2008), and they incorporate a number of calculations to summarize the relationship between stimulus and output, including spatial filtering, divisive normalization, sensitivity to second-order contrast, and nonlinear spatial summation (Kay et al. 2013b). While the model details are beyond the scope of the chapter, a few trends can be observed in the way in which model parameters differ between maps. For example, spatial summation is closest to linear in V1 and increasingly compressive (nonlinear) in visual field maps beyond V1. This pattern corresponds to the fact that in extrastriate maps like VO-1/2 or TO-1/2, even a small stimulus anywhere in the voxel receptive field produces a nearly maximal response; in V1, the response grows substantially as the spatial overlap between the stimulus and pRF gets larger. Another trend is that extrastriate maps show greater sensitivity to second-order contrast (variation in contrast level across the image) than V1, consistent with the idea that stimulus tuning becomes more complex in downstream visual areas.

PRF modeling in the human brain provides an opportunity to compare measurements made with different instruments. By using models, the comparisons can be made in model parameters that often correspond to stimulus features, like pRF location or size. This is an advantage because measurements made with different instruments such as BOLD and local field potential cannot easily be directly compared, as they have different units, different time scales, and many other differences. Comparison of pRF models made with different instruments have been informative. For example, one component of the electrical signal, an asynchronous, spectrally broadband component, is well matched to the fMRI measurement in terms of pRF position, size, and degree of spatial compression (Winawer et al. 2013). Other components of the ECoG signal, such as the amplitude of the visually evoked potential

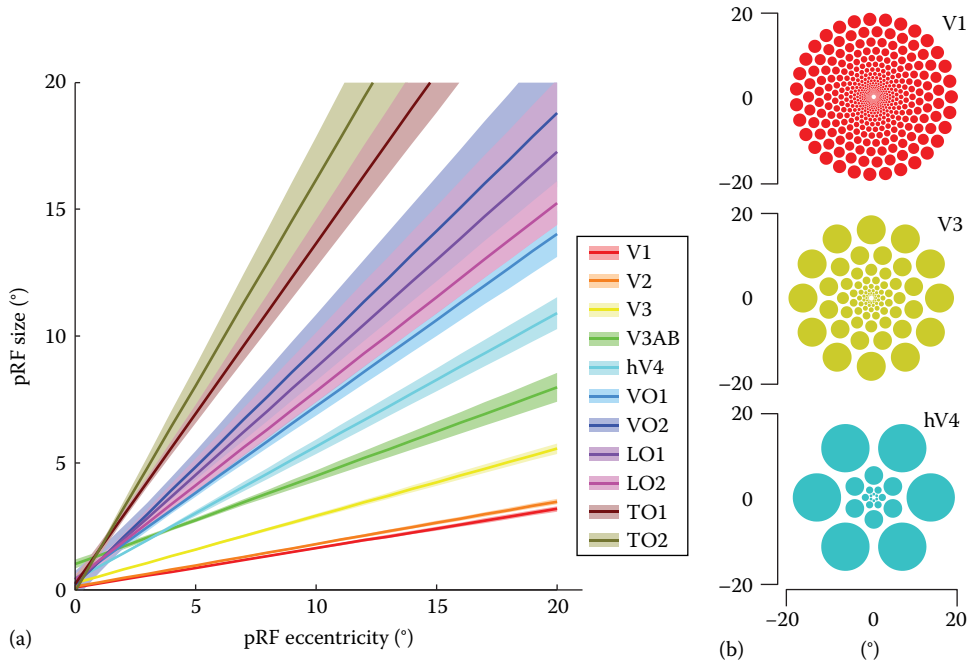

Figure 12.12 Population receptive field (pRF) size in human visual cortex. (a) pRF size is measured as a function of eccentricity and visual field map. In all visual areas, the pRF size increases with eccentricity. The pRF size is smallest in V1 (red) and increases with the visual hierarchy. The pRF size is one standard deviation of the spatial Gaussian describing the response to a point stimulus. (b) The pRF sizes of three areas are illustrated in visual space The circles are 1 standard deviation of the spatial Gaussian for a given eccentricity for each area. The images show the two trends in pRF size: larger pRFs with greater eccentricity and different pRF sizes in different visual areas. ([a]: Reproduced from Kay, K.N. et al., *J. Neurophysiol.*, 110, 481, 2013a; [b]: After Figure 1 from Freeman, J. and Simoncelli, E.P., *Nat. Neurosci.*, 14, 1195, 2011.)

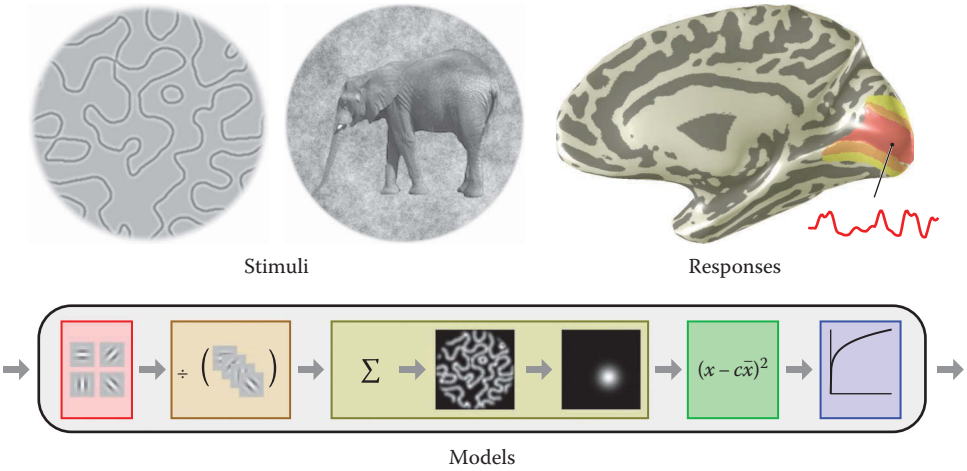

Figure 12.13 Population receptive field (PRF) modeling from pixels to BOLD. A more complete pRF model of fMRI responses takes arbitrary visual stimuli as inputs (upper left) and predicts responses in a particular location in cortex (upper right). An example of a recent model that computes predicted responses for a variety of different spatial and texture patterns is shown in the lower panel (Kay, K.N. et al. 2013b). There are several computational stages in the model, including, from left to right, filtering and rectification (red), divisive normalization (beige), spatial pooling (yellow), second-order contrast nonlinearity (green), and a spatial nonlinearity (blue). (Figure provided by Kendrick Kay, http://kendrickkay.net/socmodel/.)

or the amplitude of narrowband gamma oscillations, show different patterns, indicating that neural responses at any one cortical location contain multiple signals. In future work, models that are integrated across measurement modalities will capture more and more aspects of the circuitry and visual representation.

12.3.5.2 Functional specialization within ventral maps and visual areas

In parallel with the study of visual field maps over the last several decades, another approach has been taken to study visual cortex. This approach focuses on tasks and behaviors, as well as stimulus properties other than spatial location, in order to characterize the functional architecture of visual cortex. Several principal findings have emerged. First, the ventral stream—ventral occipital and ventral temporal cortices—contains many regions that are highly responsive to particular stimulus features. These regions include specializations for color vision, faces, words, and scenes (Figure 12.14).

Much of the knowledge about functional specialization in the ventral visual pathways is derived from a century of lesion studies by neurologists (Zeki 1993). Patients with relatively focal cortical lesions to this pathway sometimes show deficits for specific visual functions, like face or color recognition. Much as Inouye's patients with lesions to primary visual cortex were blind in certain portions of the visual field (a scotoma), patients with ventral stream lesions can became blind to certain aspects of stimuli, such as color (achromatopsia) or facial identity (prosopagnosia).

Reports of such specific blindnesses were met with skepticism by many in the field (Zeki 1990). One reason for skepticism is that the observed deficits were rarely pure; a patient with cerebral achromatopsia might also have a visual field scotoma, for example. A second reason is that it just seemed unlikely that a person could be blind to a type of stimulus rather than a portion of the visual field. Nonetheless, over time many case studies have been reported, and some of the subjects have been studied in great detail in order to carefully characterize the perceptual deficits

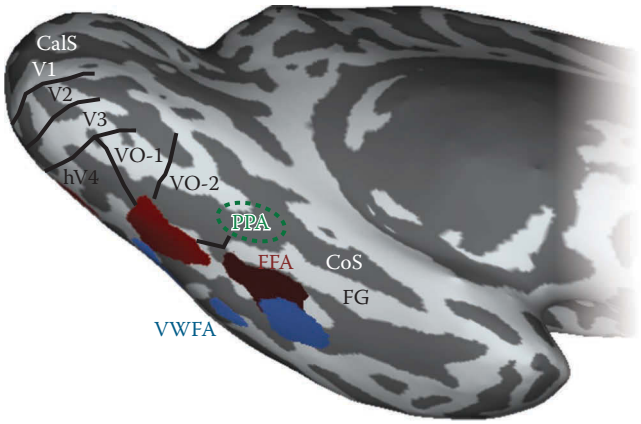

Figure 12.14 Stimulus-specific visual areas on the ventral surface of temporal cortex. A smoothed rendering of a left hemisphere, seen from below and medially, shows the locations of visual areas in ventral temporal cortex that are highly responsive to specific types of visual images. The visual word form area ("VWFA," blue) and fusiform face area ("FFA," red) were identified by functional MRI localizer experiments in which the subject viewed a variety of different stimuli; the blue and red regions were most strongly activated by images containing words or faces, respectively. Both the face- and word-selective responses comprise multiple patches (more posterior regions are filled with lighter shades), consistent with recent observations about category selective regions in ventral visual cortex (Grill-Spector and Weiner 2014, Weiner and Grill-Spector 2012). The approximate location of the parahippocampal place area ("PPA," green) is identified by comparison to previous papers. Several visual maps are shown in black outline. The PPA overlaps known visual field maps. (Adapted from a figure provided by Kendrick N. Kay, personal communication.)

(e.g., Duchaine et al. 2006). A century later, it appears that the neurologists reports were largely correct, and there are indeed locations on the ventral surface of the human visual system that show some degree of specialization for particular kinds of visual functions (Kanwisher 2010).

In the last quarter-century, functional specialization of the ventral stream has been characterized in much greater detail through the use of functional imaging with healthy subjects (PET and fMRI) and ECoG in patient volunteers (Allison et al. 1994, Grill-Spector and Weiner 2014, Kanwisher 2010). Across many studies, some patterns have become clear. First, there is a large-scale organization on the ventral temporal surface from medial to lateral (Figure 12.14). Medially, on the collateral sulcus, is a region highly responsive to scenes, sometimes called the "parahippocampal place area" (PPA) (Epstein and Kanwisher 1998). Lateral to the PPA are regions on the fusiform gyrus specialized for representing faces (Kanwisher et al. 1997). This region is sometimes called the fusiform face area (FFA), but because there may be several distinct clusters of face sensitive regions, it is also referred to by a series of anatomical names: pFus (posterior fusiform), mFus (middle fusiform), and IOG-faces (inferior occipital gyrus) (Weiner and Grill-Spector 2010). Quite close to the face area, typically slightly more laterally, is a region that is involved in seeing words, called the visual word form area (VWFA) (Ben-Shachar et al. 2007b, Cohen et al. 2000). This region is more prominent in the left hemisphere but can be identified bilaterally. More lateral are regions responsive to objects, called lateral occipital (LO) cortex (see Section 12.3.4.6) (Malach et al. 1995).

The names of these regions do not imply that the regions are *only* responsive to one kind of stimuli. The VWFA, for example, is also responsive to line drawings and many other kinds of stimuli. Nonetheless, there is enough specialization in each of these areas such that (1) they can be identified routinely in simple fMRI localizer experiments in nearly every subject based on the stimulus class that they are most responsive to and (2) cortical lesions to these locations result in perceptual deficits that are most severe in the expected domain (e.g., lesions to face areas impact face recognition more than other kinds of object recognition).

12.3.5.3 Functional specialization within lateral maps and visual areas

Several visual areas have been identified on the lateral surface of the temporal lobe. These include the areas known as "hMT+" (human middle temporal) and "LO" (lateral occipital) (Figures 12.9 and 12.10). The area known as "MT" (middle temporal) was first discovered in monkey and is a highly studied region in the visual pathways (Zeki 2004). It is a clear example of a cortical area with specialized function, in that it is highly sensitive to visual motion and binocular disparity. A neighboring region, known as MST (middle superior temporal), is also motion sensitive and appears to represent more complex forms of motion such as optic flow. The human homolog of these maps is known as hMT+ (DeYoe et al. 1994, Zeki et al. 1991). The "+" is included in the name because there are multiple visual field maps arranged in a cluster that are motion sensitive and because there is uncertainty about the exact homology between these multiple maps in human and the corresponding multiple maps in macaque. Two of these maps have been called TO-1/2 (temporal occipital 1 and 2), and they are likely homologs to MT and MST in the macaque (Amano et al. 2009, Huk et al. 2002).

Because of the very strong sensitivity to visual motion, this area can be easily identified in any human subject in a short period of fMRI scanning by contrasting the response to moving stimuli with the response to stationary stimuli. Stimulation of this region in patients with implanted electrodes causes motion illusions (Rauschecker et al. 2011), and lesions to this portion of cortex causes deficits in the ability to see visual motion ("akinetopsia") (Zeki 1991, Zihl et al. 1983). These areas are strongly modulated by top-down processes such as visual attention (Beauchamp et al. 1997).

Subsequent to the discovery of the MT maps, researchers identified an additional large visual area in the human brain, part of which was sandwiched between the early visual field maps (V1–V3) and MT and part of which extends down to the ventral surface. This area was first identified because of the functional specialization in object recognition and is generally known as LOC, the "lateral occipital complex" (Malach et al. 1995). More recently, the area has been subdivided into a more lateral and a more ventral portion (Sayres and Grill-Spector 2008). In functional MRI experiments, the LOC can be defined by having a greater response to images with intact objects compared to the same images that have been spatially scrambled in small parts. Lesions to this area cause deficits in the ability to recognize objects (object agnosia) (James et al. 2003). It was later discovered that there are two retinotopic maps between the early visual field maps (V1–V3) and MT, called LO-1 and LO-2 (Figures 12.9 and 12.10) (Larsson and Heeger 2006). The LOC overlaps LO-2.

The stimulus-selective regions of ventral and lateral occipital cortex should not be thought of as distinct from the retinotopic maps. For example, LOC, an object-selective region, overlaps the visual field map LO-2. Similarly, the PPA, a place-selective region, overlaps multiple visual field maps, including VO-2 and PHC-1/2 (Arcaro et al. 2009), and the "extrastriate body area," a region that responds to images of the human body (Epstein and Kanwisher 1998), overlaps multiple visual field maps on the dorsal surface of occipitotemporal cortex (Weiner and Grill-Spector 2011). In other cases, although maps have not yet been unambiguously identified, nonetheless there is evidence from fMRI studies that all visual regions tested to date have some sensitivity to stimulus position (Schwarzlose et al. 2008). If the position sensitivity turns out to be organized in such a way that neighboring cortical sites represent neighboring regions of visual space, then we would call the region a map. If, however, the position sensitivity does not have a clear spatial topography, then this would indicate a dissociation between spatial tuning and visual field maps. Future experiments will resolve this question in many more cortical areas such as the FFA and VWFA.

12.3.5.4 Functional specialization within dorsal maps and visual areas

Superior to the posterior maps (V1–V3), there is an ascending limb of the visual pathways including many visual field maps. Some of these maps, V3A/B, are highly responsive to visual motion and binocular disparity (Backus et al. 2001, Tootell et al. 1997). Other visual maps just superior to these, located in the intraparietal sulcus, are strongly modulated by attention (Silver et al. 2005). These maps were originally identified in memory-guided saccade tasks, in which subjects planned eye movements to locations in the visual field during fMRI scanning. For this reason, and because of the deficits associated with lesions to these maps, they are thought to play a role in coordinating visual

representations and motor movements, including eye movements. These maps are strongly modulated by visual attention.

12.3.6 CORTICAL PLASTICITY AND STABILITY

One of the most important questions about visual system architecture is how it arises in development and how it changes when there is damage or unusual inputs to the visual system. Broadly speaking, the visual system faces two competing challenges: it must maintain a stable representation of the external world, so that other cortical areas can reliably interpret the outputs, and it must have some flexibility to learn from the environment. A general finding across decades of study in humans and animal models is that very early in life, the visual system has considerable flexibility to adapt to unusual inputs and circumstances. This ability to change and adapt is called plasticity. A complementary finding is that in later development and adulthood, there is a much greater tendency toward stability, meaning that there is less plasticity. These two competing demands on the visual system, and the apparent solution of favoring plasticity in early life and stability in later life, means that congenital disorders and disorders acquired later in life result in very different outcomes (Wandell and Smirnakis 2009).

12.3.6.1 Plasticity and stability in early development

12.3.6.1.1 Bilateral visual field maps in a patient with only one hemisphere

A striking example of a congenital deficit is the case of a girl born with a missing right cerebral hemisphere (Muckli et al. 2009). Such a case poses significant challenges for the development of visual field maps. In the normal developmental trajectory, the hemidecussation in the optic nerve results in each half of visual space being represented in the contralateral hemisphere. For this reason, each of the two LGNs and V1s represent only one half of space. In this case, the visual system developed very differently. Both halves of each retina send fibers to the left (intact) hemisphere. This hemisphere, unlike in most visual systems, represents the full visual field, not just the contralateral field. In her primary visual cortex, the left and right half of visual space are represented in two maps that overlap one another. In this case study, retinal ganglion cells were rerouted from the missing (right) LGN to the intact (left) LGN, demonstrating considerable flexibility of the early developing visual system to self-organize and alter the visual system architecture.

It is interesting to contrast this result with a different case study, in which one cerebral hemisphere was lost at the age of three for treatment of chronic encephalitis and epilepsy (Haak et al. 2014). In this case, unlike the congenital case, fMRI measurements showed that the early visual maps in the intact hemisphere retained the normal organization, representing only the contralateral hemisphere. The difference between these two studies suggests that by the age of three, many parts of the visual system are much more stable (and less plastic) than earlier in development.

12.3.6.1.2 Achiasma

In the vast majority of people, the optic nerves partially cross at the optic chiasm (hemidecussation); however, there is a rare congenital disorder in which people are born with no optic chiasm. For these individuals, each eye sends retinal ganglion cell axons only to the ipsilateral LGN (no hemidecussation). Therefore, each LGN has a complete representation of the visual field from one eye, rather than a representation of one half of the visual field from two eyes. V1 inherits the unusual map from the LGN, so that each V1 represents the full visual field from one eye (Hoffmann et al. 2012, Victor et al. 2000). These individuals have an unusual visual system architecture. Similar to the case of the girl born with only one cerebral hemisphere, there appears to be a rather interesting retinotopic mapping solution for people born with no optic chiasm. They have a retinotopic map of each half of visual space folded over one other. This means that one small location in cortex represents not one contiguous region of space, but two regions that are mirror symmetric across the vertical meridian. Other than a loss of stereovision, these patients have relatively normal vision. The brain seems to learn which signals to combine and which signals to segregate; for example, even though the left and right visual field maps overlap, the subjects do not confuse inputs from the left and right half of space. This fact demonstrates that downstream visual areas, which rely on inputs from V1, have the flexibility to learn from experience how to read out an abnormal map in support of normal vision.

12.3.6.1.3 Rod monochromacy

In a rare congenital photoreceptor disorder, people are born with no functioning cones. Because the only working photoreceptors these individuals have are rods, they have no color vision and are called "rod monochromats." This poses an interesting problem for cortex and the development of the visual system architecture. Normally, the visual cortex devotes a large area to analyzing signals from the fovea; however, there are no rods in the fovea. Hence, if the cortex of rod monochromats developed like healthy controls, then there would be a large region near the occipital pole unresponsive to visual stimuli. This is not what is observed. Instead, in rod monochromats, the region of cortex that normally receives inputs from the fovea is instead responsive to rod inputs from the parafovea and periphery, reflecting plasticity in the early developing visual system (Baseler et al. 2002). It is important to note that this cortical response does not provide any vision at the fovea; after all, if there is no light absorption there can be no vision. What the plasticity means is that a certain portion of cortex functions differently in these individuals, contributing to visual analysis of signals originating outside the fovea.

12.3.6.2 Plasticity and stability in late development and adulthood

12.3.6.2.1 Retinal disorders (AMD/JMD, RP)

The effect of retinal disorders on brain function differs when the disorder happens later in life compared to when it is congenital, as in rod monochromacy. In several disorders, such as juvenile and age-related macular degeneration and retinitis pigmentosa, photoreceptors degenerate or become nonfunctional in a portion of the retina, creating a scotoma in the visual field, and a corresponding "lesion projection zone" in the cortex (Figure 12.15). In macular degeneration, the scotoma is in the central retina, and in retinitis pigmentosa, the scotoma is in the periphery. Because these disorders emerge well after the critical period in development, the brain shows little plasticity despite the rather

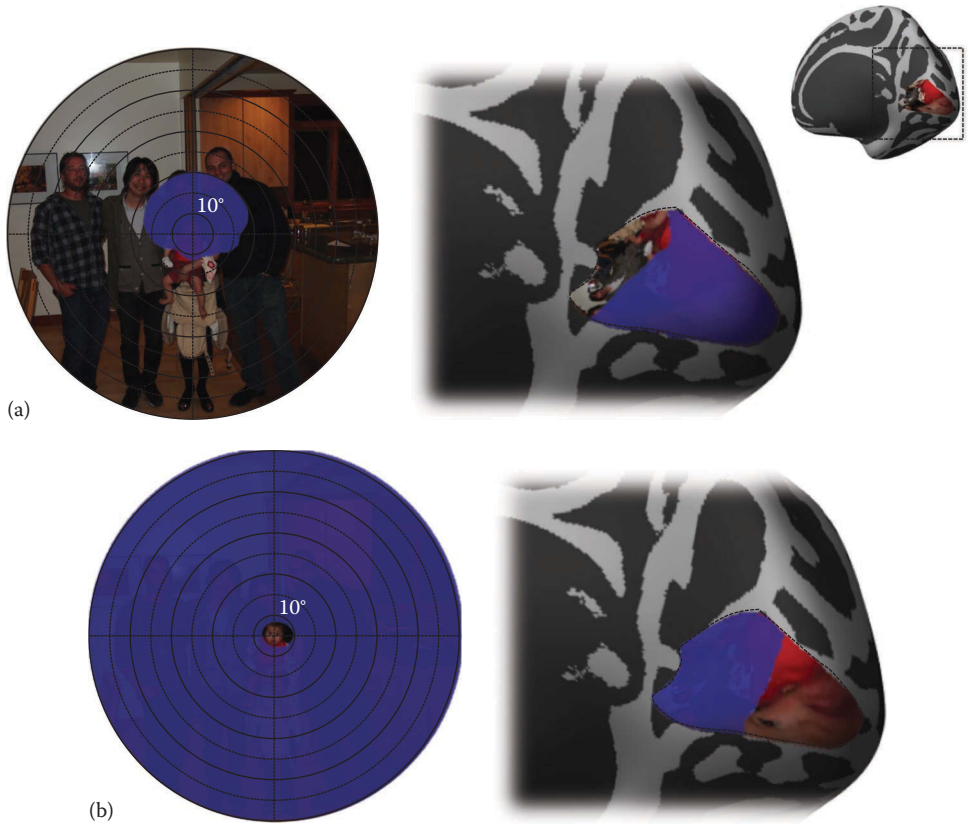

Figure 12.15 Retinal lesions. Various retinal diseases cause loss of function in regions of the retina. (a) The left panel shows an example of visual field loss from juvenile macular degeneration (JMD). The visual field loss is colored blue and is superimposed on an image (maximum visual angle of 90°). The cortical mesh on the right shows the projection of the image onto primary visual cortex. The lesion projection zone in blue. (b) An example of retinitis pigmentosa (RP), in which only a small central portion of the visual field is intact. All of the periphery indicates visual field loss (blue). The cortical mesh again shows the projection of the image onto primary visual cortex, with the lesion projection zone in blue. Note that the visual field loss is much larger in the case of the RP patient, but the cortical lesion projection zone is much larger for the JMD patient.

large changes in inputs associated with the diseases. As a result, large regions of visual cortex become relatively unresponsive to visual inputs (Baseler et al. 2011, Wandell and Smirnakis 2009). Because these visual areas were once functional, they can still be activated by feedback signals from higher brain regions, such as during memory or attention (Baker et al. 2005, Masuda et al. 2008, 2010).

12.3.6.2.2 Image restoration late in life

A question popular among philosophers is whether a person who has lived his or her life blind could learn to interpret images late in life if sight were restored. Such a situation has occasionally been borne out in the clinic. One case is the patient Mike May, who was blinded in a chemical accident at age 3 and remained blind until a corneal transplant surgery at age 46. Normally, the visual system is not fully mature by age 3. This means that when Mike lost his sight, his visual system was still developing. The development presumably stopped at this point so that when his retinal image was surgically repaired as an adult, his visual system was not fully mature. A key question was whether his visual system could mature at this late age, rendering a normal cortical architecture and visual perception. The answer, it seems, is no. Despite a clear image at the retina, even 10 years after surgery, his vision was still significantly impaired, and measurements of his retinotopic maps, pRFs, and major fiber tracts all showed substantial differences from healthy controls (Fine et al. 2003, Levin et al. 2010). This case study indicates the limits of plasticity later in life.

12.4 SUMMARY

The visual system architecture reflects the wide array of functions the system performs, ranging from sensory to motor to circadian. All visual function originates with signals in the retina, processed by numerous cell types, including multiple classes of photoreceptors and ganglion cells. Signals leaving the eye are routed through a single nerve bundle, the optic nerve, which branches and targets numerous subcortical nuclei. Several important features of the visual system are exemplified in the branching pattern: (1) In hemidecussation, signals are separated by visual field, projecting to the contralateral hemisphere. (2) In parallel pathways, signals are segregated by cell type and eye of origin. The outputs of parallel pathways are then recombined to form new pathways. (3) In retinotopy, signals are represented by nearby points in the visual field project to nearby end points in the brain.

The visual pathways support many functions, ranging from circadian to motor to perception. The largest pathway is the geniculostriate pathway, in which signals are conveyed from

retina to thalamus to cortex. Primary visual cortex, the largest recipient of visual fibers from the thalamus, distributes signals to many other areas of visual cortex. Most of these areas preserve the visual field map and are arranged in clusters of two or more maps. The different clusters emphasize different aspects of the stimulus and behavior. The more dorsal clusters contribute to spatial representations, spatial attention, and eye movements. The more ventral and lateral clusters contribute to recognition and appearance. Tools for studying these areas in the human brain have improved dramatically in the last few decades, allowing researchers to measure and quantitatively model the responses in many portions of the visual system as well as to measure the tissue properties of gray and white matter and fiber pathways connecting the visual areas. Studies of plasticity show that when inputs or pathways are abnormal early in development, there can be large changes to how the visual system develops.

ACKNOWLEDGMENTS

We thank Jennifer M Yoon, Kevin Weiner, and Brian Wandell for reading this chapter and providing many helpful suggestions.

REFERENCES

Adams, D. L., L. C. Sincich, and J. C. Horton. 2007. Complete pattern of ocular dominance columns in human primary visual cortex. *J Neurosci* 27 (39):10391–10403. doi: 10.1523/JNEUROSCI.2923-07.2007.

Allison, T., G. McCarthy, A. Nobre, A. Puce, and A. Belger. 1994. Human extrastriate visual cortex and the perception of faces, words, numbers, and colors. *Cereb Cortex* 4 (5):544–554.

Amano, K., B. A. Wandell, and S. O. Dumoulin. 2009. Visual field maps, population receptive field sizes, and visual field coverage in the human MT+ complex. *J Neurophysiol* 102 (5):2704–2718. doi: 10.1152/jn.00102.2009.

Andrews, T. J., S. D. Halpern, and D. Purves. 1997. Correlated size variations in human visual cortex, lateral geniculate nucleus, and optic tract. *J Neurosci* 17 (8):2859–2868.

Arcaro, M. J., S. A. McMains, B. D. Singer, and S. Kastner. 2009. Retinotopic organization of human ventral visual cortex. *J Neurosci* 29 (34):10638–10652.

Backus, B. T., D. J. Fleet, A. J. Parker, and D. J. Heeger. 2001. Human cortical activity correlates with stereoscopic depth perception. *J Neurophysiol* 86 (4):2054–2068.

Baker, C. I., E. Peli, N. Knouf, and N. G. Kanwisher. 2005. Reorganization of visual processing in macular degeneration. *J Neurosci* 25 (3):614–618. doi: 10.1523/JNEUROSCI.3476-04.2005.

Baseler, H. A., A. A. Brewer, L. T. Sharpe, A. B. Morland, H. Jagle, and B. A. Wandell. 2002. Reorganization of human cortical maps caused by inherited photoreceptor abnormalities. *Nat Neurosci* 5 (4):364–370. doi: 10.1038/nn817.

Baseler, H. A., A. Gouws, K. V. Haak, C. Racey, M. D. Crossland, A. Tufail, G. S. Rubin, F. W. Cornelissen, and A. B. Morland. 2011. Large-scale remapping of visual cortex is absent in adult humans with macular degeneration. *Nat Neurosci* 14 (5):649–655. doi: 10.1038/nn.2793.

Beauchamp, M. S., R. W. Cox, and E. A. DeYoe. 1997. Graded effects of spatial and featural attention on human area MT and associated motion processing areas. *J Neurophysiol* 78 (1):516–520.

Ben-Shachar, M., R. F. Dougherty, and B. A. Wandell. 2007a. White matter pathways in reading. *Curr Opin Neurobiol* 17 (2):258–270.

Ben-Shachar, M., R. F. Dougherty, G. K. Deutsch, and B. A. Wandell. 2007b. Differential sensitivity to words and shapes in ventral occipito-temporal cortex. *Cereb Cortex* 17 (7):1604–1611.

Benson, N. C., O. H. Butt, D. H. Brainard, and G. K. Aguirre. 2014. Correction of distortion in flattened representations of the cortical surface allows prediction of V1-V3 functional organization from anatomy. *PLoS Comput Biol* 10 (3):e1003538. doi: 10.1371/journal.pcbi.1003538.

Benson, N. C., O. H. Butt, R. Datta, P. D. Radoeva, D. H. Brainard, and G. K. Aguirre. 2012. The retinotopic organization of striate cortex is well predicted by surface topology. *Curr Biol* 22 (21):2081–2085. doi: 10.1016/j.cub.2012.09.014.

Berson, D. M., F. A. Dunn, and M. Takao. 2002. Phototransduction by retinal ganglion cells that set the circadian clock. *Science* 295 (5557):1070–1073. doi: 10.1126/science.1067262.

Brewer, A. A., J. Liu, A. R. Wade, and B. A. Wandell. 2005. Visual field maps and stimulus selectivity in human ventral occipital cortex. *Nat Neurosci* 8 (8):1102–1109.

Brewster, D. 1860. *Memoirs of the Life, Writings, and Discoveries of Sir Isaac Newton: 2*, Vol. 2. Edmonston and Douglas, London, U.K.

Carandini, M., J. B. Demb, V. Mante, D. J. Tolhurst, Y. Dan, B. A. Olshausen, J. L. Gallant, and N. C. Rust. 2005. Do we know what the early visual system does? *J Neurosci* 25 (46):10577–10597. doi: 10.1523/JNEUROSCI.3726-05.2005.

Cardin, V., R. Sherrington, L. Hemsworth, and A. T. Smith. 2012. Human V6: Functional characterisation and localisation. *PLoS One* 7 (10):e47685. doi: 10.1371/journal.pone.0047685.

Cohen, L., S. Dehaene, L. Naccache, S. Lehericy, G. Dehaene-Lambertz, M. A. Henaff, and F. Michel. 2000. The visual word form area: Spatial and temporal characterization of an initial stage of reading in normal subjects and posterior split-brain patients. *Brain* 123 (Pt 2):291–307.

Connolly, M. and D. Van Essen. 1984. The representation of the visual field in parvicellular and magnocellular layers of the lateral geniculate nucleus in the macaque monkey. *J Comp Neurol* 226 (4):544–564. doi: 10.1002/cne.902260408.

Dacey, D. M. 1993. The mosaic of midget ganglion cells in the human retina. *J Neurosci* 13 (12):5334–5355.

Dayan, M., M. Munoz, S. Jentschke, M. J. Chadwick, J. M. Cooper, K. Riney, F. Vargha-Khadem, and C. A. Clark. 2013. Optic radiation structure and anatomy in the normally developing brain determined using diffusion MRI and tractography. *Brain Struct Funct*. doi: 10.1007/s00429-013-0655-y.

Denison, R. N., A. T. Vu, E. Yacoub, D. A. Feinberg, and M. A. Silver. 2014. Functional mapping of the magnocellular and parvocellular subdivisions of human LGN. *Neuroimage* 102P2:358–369. doi: 10.1016/j.neuroimage.2014.07.019.

DeYoe, E. A., P. Bandettini, J. Neitz, D. Miller, and P. Winans. 1994. Functional magnetic resonance imaging (FMRI) of the human brain. *J Neurosci Methods* 54 (2):171–187.

Dougherty, R. F., V. M. Koch, A. A. Brewer, B. Fischer, J. Modersitzki, and B. A. Wandell. 2003. Visual field representations and locations of visual areas V1/2/3 in human visual cortex. *J Vis* 3 (10):586–598. doi: 10:1167/3.10.1.

Drager, U. C. and J. F. Olsen. 1980. Origins of crossed and uncrossed retinal projections in pigmented and albino mice. *J Comp Neurol* 191 (3):383–412. doi: 10.1002/cne.901910306.

Duchaine, B. C., G. Yovel, E. J. Butterworth, and K. Nakayama. 2006. Prosopagnosia as an impairment to face-specific mechanisms: Elimination of the alternative hypotheses in a developmental case. *Cogn Neuropsychol* 23 (5):714–747. doi: 10.1080/02643290500441296.

Dumoulin, S. O., R. D. Hoge, C. L. Baker, Jr., R. F. Hess, R. L. Achtman, and A. C. Evans. 2003. Automatic volumetric segmentation of human visual retinotopic cortex. *Neuroimage* 18 (3):576–587.

Dumoulin, S. O. and B. A. Wandell. 2008. Population receptive field estimates in human visual cortex. *Neuroimage* 39 (2):647–660. doi: 10.1016/j.neuroimage.2007.09.034.

Engel, S. A., G. H. Glover, and B. A. Wandell. 1997. Retinotopic organization in human visual cortex and the spatial precision of functional MRI. *Cerebral Cortex* 7 (2):181–192.

Engel, S. A., D. E. Rumelhart, B. A. Wandell, A. T. Lee, G. H. Glover, E. J. Chichilnisky, and M. N. Shadlen. 1994. fMRI of human visual cortex. *Nature* 369 (6481):525. doi: 10.1038/369525a0.

Epstein, R. and N. Kanwisher. 1998. A cortical representation of the local visual environment. *Nature* 392 (6676):598–601.

Felleman, D. J. and D. C. Van Essen. 1991. Distributed hierarchical processing in the primate cerebral cortex. *Cereb Cortex* 1 (1):1–47.

Field, G. D. and E. J. Chichilnisky. 2007. Information processing in the primate retina: Circuitry and coding. *Annu Rev Neurosci* 30:1–30. doi: 10.1146/annurev.neuro.30.051606.094252.

Fine, I., A. R. Wade, A. A. Brewer, M. G. May, D. F. Goodman, G. M. Boynton, B. A. Wandell, and D. I. MacLeod. 2003. Long-term deprivation affects visual perception and cortex. *Nat Neurosci* 6 (9):915–916.

Fitzgibbon, T. and S. F. Taylor. 1996. Retinotopy of the human retinal nerve fibre layer and optic nerve head. *J Comp Neurol* 375 (2):238–251. doi: 10.1002/(SICI)1096-9861(19961111)375:2<238::AID-CNE5>3.0.CO;2-3.

Flechsig, P. 1901. Developmental (myelogenetic) localisation of the cerebral cortex in the human subject. *Lancet* 158 (4077):1027–1030.

Flynn-Evans, E. E., H. Tabandeh, D. J. Skene, and S. W. Lockley. 2014. Circadian rhythm disorders and melatonin production in 127 blind women with and without light perception. *J Biol Rhythms* 29 (3):215–224. doi: 10.1177/0748730414536852.

Freeman, J. and E. P. Simoncelli. 2011. Metamers of the ventral stream. *Nat Neurosci* 14 (9):1195–1201. doi: 10.1038/nn.2889.

Grill-Spector, K., T. Kushnir, T. Hendler, S. Edelman, Y. Itzchak, and R. Malach. 1998. A sequence of object-processing stages revealed by fMRI in the human occipital lobe. *Hum Brain Mapp* 6 (4):316–328.

Grill-Spector, K. and K. S. Weiner. 2014. The functional architecture of the ventral temporal cortex and its role in categorization. *Nat Rev Neurosci* 15 (8):536–548. doi: 10.1038/nrn3747.

Haak, K. V., D. R. Langers, R. Renken, P. van Dijk, J. Borgstein, and F. W. Cornelissen. 2014. Abnormal visual field maps in human cortex: A mini-review and a case report. *Cortex* 56:14–25. doi: 10.1016/j.cortex.2012.12.005.

Harvey, B. M., M. J. Vansteensel, C. H. Ferrier, N. Petridou, W. Zuiderbaan, E. J. Aarnoutse, M. G. Bleichner et al. 2012. Frequency specific spatial interactions in human electrocorticography: V1 alpha oscillations reflect surround suppression. *NeuroImage*. doi: 10.1016/j.neuroimage.2012.10.020.

Heeger, D. J., E. P. Simoncelli, and J. A. Movshon. 1996. Computational models of cortical visual processing. *Proc Natl Acad Sci U S A* 93 (2):623–627.

Henschen, S.E. 1893. On the visual path and centre. *Brain* 16 (1–2):170–180.

Hofbauer, A. and U. C. Drager. 1985. Depth segregation of retinal ganglion cells projecting to mouse superior colliculus. *J Comp Neurol* 234 (4):465–474. doi: 10.1002/cne.902340405.

Hoffmann, M. B., F. R. Kaule, N. Levin, Y. Masuda, A. Kumar, I. Gottlob, H. Horiguchi, R. F. Dougherty et al. 2012. Plasticity and stability of the visual system in human achiasma. *Neuron* 75 (3):393–401. doi: 10.1016/j.neuron.2012.05.026.

Holmes, G. 1918. Disturbances of vision by cerebral lesions. *Br J Ophthalmol* 2 (7):353–384.

Holmes, G. and W. T. Lister. 1916. Disturbances of vision from cerebral lesions, with special reference to the cortical representation of the macula. *Brain* 39 (1–2):34–73.

Horton, J. C., M. M. Greenwood, and D. H. Hubel. 1979. Non-retinotopic arrangement of fibres in cat optic nerve. *Nature* 282 (5740):720–722.

Horton, J. C. and E. T. Hedley-Whyte. 1984. Mapping of cytochrome oxidase patches and ocular dominance columns in human visual cortex. *Philos Trans R Soc Lond B Biol Sci* 304 (1119):255–272.

Horton, J. C. and W. F. Hoyt. 1991a. Quadrantic visual field defects. A hallmark of lesions in extrastriate (V2/V3) cortex. *Brain* 114 (Pt 4):1703–1718.

Horton, J. C. and W. F. Hoyt. 1991b. The representation of the visual field in human striate cortex. A revision of the classic Holmes map. *Arch Ophthalmol* 109 (6):816–824.

Hubel, D. H. and T. N. Wiesel. 1977. Ferrier lecture. Functional architecture of macaque monkey visual cortex. *Proc R Soc Lond B Biol Sci* 198 (1130):1–59.

Hubel, D. H., T. N. Wiesel, and S. LeVay. 1977. Plasticity of ocular dominance columns in monkey striate cortex. *Philos Trans R Soc Lond B Biol Sci* 278 (961):377–409.

Huk, A. C., R. F. Dougherty, and D. J. Heeger. 2002. Retinotopy and functional subdivision of human areas MT and MST. *J Neurosc* 22 (16):7195–7205.

Inouye, T. 2000. Eye disturbances after gunshot injuries to the cortical visual pathways. Translated from the German by Glickstein M, and Fahle M. Oxford University Press, Oxford, U.K.

James, T. W., J. Culham, G. K. Humphrey, A. D. Milner, and M. A. Goodale. 2003. Ventral occipital lesions impair object recognition but not object-directed grasping: An fMRI study. *Brain* 126 (Pt 11):2463–2475. doi: 10.1093/brain/awg248.

Jerde, T. A. and C. E. Curtis. 2013. Maps of space in human frontoparietal cortex. *J Physiol Paris* 107 (6):510–516. doi: 10.1016/j.jphysparis.2013.04.002.

Jerde, T. A., E. P. Merriam, A. C. Riggall, J. H. Hedges, and C. E. Curtis. 2012. Prioritized maps of space in human frontoparietal cortex. *J Neurosci* 32 (48):17382–17390. doi: 10.1523/JNEUROSCI.3810-12.2012.

Kandel, E.R., James, H. S., and Thomas, M. J. 2000. *Principles of Neural Science*, Vol. 4. McGraw-Hill, New York.

Kanwisher, N. 2010. Functional specificity in the human brain: A window into the functional architecture of the mind. *Proc Natl Acad Sci U S A* 107 (25):11163–11170. doi: 10.1073/pnas.1005062107.

Kanwisher, N., J. McDermott, and M. M. Chun. 1997. The fusiform face area: A module in human extrastriate cortex specialized for face perception. *J Neurosci* 17 (11):4302–4311.

Kastner, S., K. A. Schneider, and K. Wunderlich. 2006. Beyond a relay nucleus: Neuroimaging views on the human LGN. *Prog Brain Res* 155:125–143. doi: 10.1016/S0079-6123(06)55008-3.

Katyal, S., S. Zughni, C. Greene, and D. Ress. 2010. Topography of covert visual attention in human superior colliculus. *J Neurophysiol* 104 (6):3074–3083. doi: 10.1152/jn.00283.2010.

Kay, K. N., T. Naselaris, R. J. Prenger, and J. L. Gallant. 2008. Identifying natural images from human brain activity. *Nature* 452 (7185):352–355. doi: 10.1038/nature06713.

Kay, K. N., J. Winawer, A. Mezer, and B. A. Wandell. 2013a. Compressive spatial summation in human visual cortex. *J Neurophysiol* 110 (2):481–494. doi: 10.1152/jn.00105.2013.

Kay, K. N., J. Winawer, A. Rokem, A. Mezer, and B. A. Wandell. 2013b. A two-stage cascade model of BOLD responses in human visual cortex. *PLoS Comput Biol* 9 (5):e1003079. doi: 10.1371/journal.pcbi.1003079.

Kinney, H. C., B. A. Brody, A. S. Kloman, and F. H. Gilles. 1988. Sequence of central nervous system myelination in human infancy. II. Patterns of myelination in autopsied infants. *J Neuropathol Exp Neurol* 47 (3):217–234.

Kiorpes, L. and S. P. McKee. 1999. Neural mechanisms underlying amblyopia. *Curr Opin Neurobiol* 9 (4):480–486.

Kolster, H., J. B. Mandeville, J. T. Arsenault, L. B. Ekstrom, L. L. Wald, and W. Vanduffel. 2009. Visual field map clusters in macaque extrastriate visual cortex. *J Neurosci* 29 (21):7031–7039. doi: 10.1523/JNEUROSCI.0518-09.2009.

Larsson, J. and D. J. Heeger. 2006. Two retinotopic visual areas in human lateral occipital cortex. *J Neurosci* 26 (51):13128–13142.

Levin, N., S. O. Dumoulin, J. Winawer, R. F. Dougherty, and B. A. Wandell. 2010. Cortical maps and white matter tracts following long period of visual deprivation and retinal image restoration. *Neuron* 65 (1):21–31. doi: 10.1016/j.neuron.2009.12.006.

Malach, R., J. B. Reppas, R. R. Benson, K. K. Kwong, H. Jiang, W. A. Kennedy, P. J. Ledden, T. J. Brady, B. R. Rosen, and R. B. Tootell. 1995. Object-related activity revealed by functional magnetic resonance imaging in human occipital cortex. *Proc Natl Acad Sci U S A* 92 (18):8135–8139.

Masuda, Y., S. O. Dumoulin, S. Nakadomari, and B. A. Wandell. 2008. V1 projection zone signals in human macular degeneration depend on task, not stimulus. *Cereb Cortex* 18 (11):2483–2493.

Masuda, Y., H. Horiguchi, S. O. Dumoulin, A. Furuta, S. Miyauchi, S. Nakadomari, and B. A. Wandell. 2010. Task-dependent V1 responses in human retinitis pigmentosa. *Invest Ophthalmol Vis Sci* 51 (10):5356–5364. doi: 10.1167/iovs.09-4775.

Maunsell, J. H. and W. T. Newsome. 1987. Visual processing in monkey extrastriate cortex. *Ann Rev Neurosc* 10:363–401.

Mezer, A., J. D. Yeatman, N. Stikov, K. N. Kay, N. J. Cho, R. F. Dougherty, M. L. Perry et al. 2013. Quantifying the local tissue volume and composition in individual brains with magnetic resonance imaging. *Nat Med* 19 (12):1667–1672. doi: 10.1038/nm.3390.

Muckli, L., M. J. Naumer, and W. Singer. 2009. Bilateral visual field maps in a patient with only one hemisphere. *Proc Natl Acad Sci U S A* 106 (31):13034–13039. doi: 10.1073/pnas.0809688106.

Perry, V. H., R. Oehler, and A. Cowey. 1984. Retinal ganglion cells that project to the dorsal lateral geniculate nucleus in the macaque monkey. *Neuroscience* 12 (4):1101–1123.

Pitzalis, S., C. Galletti, R. S. Huang, F. Patria, G. Committeri, G. Galati, P. Fattori, and M. I. Sereno. 2006. Wide-field retinotopy defines human cortical visual area v6. *J Neurosci* 26 (30):7962–7973. doi: 10.1523/JNEUROSCI.0178-06.2006.

Provencio, I., I. R. Rodriguez, G. Jiang, W. P. Hayes, E. F. Moreira, and M. D. Rollag. 2000. A novel human opsin in the inner retina. *J Neurosci* 20 (2):600–605.

Prusky, G. T. and R. M. Douglas. 2004. Characterization of mouse cortical spatial vision. *Vision Res* 44 (28):3411–3418. doi: 10.1016/j.visres.2004.09.001.

Rauschecker, A. M., M. Dastjerdi, K. S. Weiner, N. Witthoft, J. Chen, A. Selimbeyoglu, and J. Parvizi. 2011. Illusions of visual motion elicited by electrical stimulation of human MT complex. *PLoS One* 6 (7):e21798. doi: 10.1371/journal.pone.0021798.

Riesenhuber, M. and T. Poggio. 1999. Hierarchical models of object recognition in cortex. *Nat Neurosc* 2 (11):1019–1025.

Sayres, R. and K. Grill-Spector. 2008. Relating retinotopic and object-selective responses in human lateral occipital cortex. *J Neurophysiol* 100 (1):249–267.

Schira, M. M., C. W. Tyler, M. Breakspear, and B. Spehar. 2009. The foveal confluence in human visual cortex. *J Neurosci* 29 (28):9050–9058.

Schneider, K. A. and S. Kastner. 2005. Visual responses of the human superior colliculus: A high-resolution functional magnetic resonance imaging study. *J Neurophysiol* 94 (4):2491–2503. doi: 10.1152/jn.00288.2005.

Schneider, K. A., M. C. Richter, and S. Kastner. 2004. Retinotopic organization and functional subdivisions of the human lateral geniculate nucleus: A high-resolution functional magnetic resonance imaging study. *J Neurosci* 24 (41):8975–8985. doi: 10.1523/JNEUROSCI.2413-04.2004.

Schwarzlose, R. F., J. D. Swisher, S. Dang, and N. Kanwisher. 2008. The distribution of category and location information across object-selective regions in human visual cortex. *Proc Natl Acad Sci U S A* 105 (11):4447–4452. doi: 10.1073/pnas.0800431105.

Sereno, M. I., A. M. Dale, J. B. Reppas, K. K. Kwong, J. W. Belliveau, T. J. Brady, B. R. Rosen, and R. B. Tootell. 1995. Borders of multiple visual areas in humans revealed by functional magnetic resonance imaging. *Science* 268 (5212):889–893.

Sereno, M. I. and R. B. Tootell. 2005. From monkeys to humans: What do we now know about brain homologies? *Curr Opin Neurobiol* 15 (2):135–144. doi: 10.1016/j.conb.2005.03.014.

Shapley, R. and M. Hawken. 2002. Neural mechanisms for color perception in the primary visual cortex. *Curr Opin Neurobiol* 12 (4):426–432.

Sherman, S. M. 2007. The thalamus is more than just a relay. *Curr Opin Neurobiol* 17 (4):417–422. doi: 10.1016/j.conb.2007.07.003.

Sherman, S. M. and C. Koch. 1986. The control of retinogeniculate transmission in the mammalian lateral geniculate nucleus. *Exp Brain Res* 63 (1):1–20.

Sillito, A. M. and H. E. Jones. 2002. Corticothalamic interactions in the transfer of visual information. *Philos Trans R Soc Lond B Biol Sci* 357 (1428):1739–1752. doi: 10.1098/rstb.2002.1170.

Silver, M. A., D. Ress, and D. J. Heeger. 2005. Topographic maps of visual spatial attention in human parietal cortex. *J Neurophysiol* 94 (2):1358–1371. doi: 10.1152/jn.01316.2004.

Snow, J. C., H. A. Allen, R. D. Rafal, and G. W. Humphreys. 2009. Impaired attentional selection following lesions to human pulvinar: Evidence for homology between human and monkey. *Proc Natl Acad Sci U S A* 106 (10):4054–4059. doi: 10.1073/pnas.0810086106.

Stein, B. E., M. W. Wallace, T. R. Stanford, and W. Jiang. 2002. Cortex governs multisensory integration in the midbrain. *Neuroscientist* 8 (4):306–314.

Stenbacka, L. and S. Vanni. 2007. fMRI of peripheral visual field representation. *Clin Neurophysiol* 118 (6):1303–1314. doi: 10.1016/j.clinph.2007.01.023.

Stensaas, S. S., D. K. Eddington, and W. H. Dobelle. 1974. The topography and variability of the primary visual cortex in man. *J Neurosurg* 40 (6):747–755. doi: 10.3171/jns.1974.40.6.0747.

Swisher, J. D., M. A. Halko, L. B. Merabet, S. A. McMains, and D. C. Somers. 2007. Visual topography of human intraparietal sulcus. *J Neurosci* 27 (20):5326–5337. doi: 10.1523/JNEUROSCI.0991-07.2007.

Tootell, R. B., J. D. Mendola, N. K. Hadjikhani, P. J. Ledden, A. K. Liu, J. B. Reppas, M. I. Sereno, and A. M. Dale. 1997. Functional analysis of V3A and related areas in human visual cortex. *J Neurosci* 17 (18):7060–7078.

Ungerleider, L. G. and J. V. Haxby. 1994. 'What' and 'where' in the human brain. *Curr Opin Neurobiol* 4 (2):157–165.

Ungerleider, L. G. and M. Mishkin. 1982. Two cortical visual systems. In *Analysis of Visual Behavior*, eds. D. Ingle, M. A. Goodale, and R. J. W. Mansfield, pp. 549–587. MIT Press, Cambridge, MA.

Van Essen, D. C. 2004. Organization of visual areas in macaque and human cerebral cortex. In *The Visual Neurosciences*, eds. L. M. Chalupa and J. S. Werner, pp. 507–521. MIT Press, Cambridge, MA.

Victor, J. D., P. Apkarian, J. Hirsch, M. M. Conte, M. Packard, N. R. Relkin, K. H. Kim, and R. M. Shapley. 2000. Visual function and brain organization in non-decussating retinal-fugal fibre syndrome. *Cereb Cortex* 10 (1):2–22.

Victor, J. D., K. Purpura, E. Katz, and B. Mao. 1994. Population encoding of spatial frequency, orientation, and color in macaque V1. *J Neurophysiol* 72 (5):2151–2166.

Wandell, B. A., A. A. Brewer, and R. F. Dougherty. 2005. Visual field map clusters in human cortex. *Philos Trans R Soc Lond B Biol Sci* 360 (1456):693–707.

Wandell, B. A., S. O. Dumoulin, and A. A. Brewer. 2007. Visual field maps in human cortex. *Neuron* 56 (2):366–383.

Wandell, B. A. and S. M. Smirnakis. 2009. Plasticity and stability of visual field maps in adult primary visual cortex. *Nat Rev Neurosci* 10 (12):873–884. doi: 10.1038/nrn2741.

Wandell, B. A. and J. Winawer. 2011. Imaging retinotopic maps in the human brain. *Vis Res* 51 (7):718–737. doi: 10.1016/j.visres.2010.08.004.

Wandell, B. A., J. Winawer, and K. N. Kay. 2015. Computational modeling of responses in human visual cortex. In *Brain Mapping: An Encyclopedic Reference*, ed. A. Toga.

Wandell, B. A. and J. D. Yeatman. 2013. Biological development of reading circuits. *Curr Opin Neurobiol* 23 (2):261–268. doi: 10.1016/j.conb.2012.12.005.

Wandell, B. A. 1995. *Foundations of Vision*. Sinauer Associates, Sunderland, MA.

Weiner, K. S. and K. Grill-Spector. 2010. Sparsely-distributed organization of face and limb activations in human ventral temporal cortex. *Neuroimage* 52 (4):1559–1573. doi: 10.1016/j.neuroimage.2010.04.262.

Weiner, K. S. and K. Grill-Spector. 2011. Not one extrastriate body area: Using anatomical landmarks, hMT+, and visual field maps to parcellate limb-selective activations in human lateral occipitotemporal cortex. *Neuroimage* 56 (4):2183–2199. doi: 10.1016/j.neuroimage.2011.03.041.

Weiner, K. S. and K. Grill-Spector. 2012. The improbable simplicity of the fusiform face area. *Trends Cogn Sci* 16 (5):251–254. doi: 10.1016/j.tics.2012.03.003.

Winawer, J., H. Horiguchi, R. A. Sayres, K. Amano, and B. A. Wandell. 2010. Mapping hV4 and ventral occipital cortex: The venous eclipse. *J Vis* 10 (5):1. doi: 10.1167/10.5.1.

Winawer, J., K. N. Kay, B. L. Foster, A. M. Rauschecker, J. Parvizi, and B. A. Wandell. 2013. Asynchronous broadband signals are the principal source of the BOLD response in human visual cortex. *Curr Biol* 23 (13):1145–1153. doi: 10.1016/j.cub.2013.05.001.

Witthoft, N., M. L. Nguyen, G. Golarai, K. F. LaRocque, A. Liberman, M. E. Smith, and K. Grill-Spector, 2014. Where is human V4? Predicting the location of hV4 and VO1 from cortical folding. *Cereb Cortex* 24 (9):2401–2408. doi:10.1093/cercor/bht092.

Yeatman, J. D., A. M. Rauschecker, and B. A. Wandell. 2013. Anatomy of the visual word form area: Adjacent cortical circuits and long-range white matter connections. *Brain Lang* 125 (2):146–155. doi: 10.1016/j.bandl.2012.04.010.

Yeatman, J. D., B. A. Wandell, and A. A. Mezer. 2014. Lifespan maturation and degeneration of human brain white matter. *Nat Commun* 5:4932. doi: 10.1038/ncomms5932.

Yoshor, D., G. M. Ghose, W. H. Bosking, P. Sun, and J. H. Maunsell. 2007. Spatial attention does not strongly modulate neuronal responses in early human visual cortex. *J Neurosc: Off J Soc Neurosc* 27 (48):13205–13209. doi: 10.1523/JNEUROSCI.2944-07.2007.

Zeki, S. 1990. A century of cerebral achromatopsia. *Brain* 113 (Pt 6): 1721–1777.

Zeki, S. 1991. Cerebral akinetopsia (visual motion blindness). A review. *Brain* 114 (Pt 2):811–824.

Zeki, S. 1993. *A Vision of the Brain*. Blackwell Scientific Publications, Oxford, U.K.

Zeki, S. 2004. Thirty years of a very special visual area, Area V5. *J Physiol* 557 (Pt 1):1–2. doi: 10.1113/jphysiol.2004.063040.

Zeki, S., J. D. Watson, C. J. Lueck, K. J. Friston, C. Kennard, and R. S. Frackowiak. 1991. A direct demonstration of functional specialization in human visual cortex. *J Neurosci* 11 (3):641–649.

Zihl, J., D. von Cramon, and N. Mai. 1983. Selective disturbance of movement vision after bilateral brain damage. *Brain* 106 (Pt 2):313–340.